

Review

A Brief Introduction and Current State of Polyvinylidene Fluoride as an Energy Harvester

Nikola Papež¹ , Tatiana Pisarenko¹ , Erik Ščasnovič² , Dinara Sobola^{1,3,†} , Ștefan Țălu^{4,*} , Rashid Dallaev¹ , Klára Částková^{2,5,‡}  and Petr Sedlák¹ 

¹ Department of Physics, Faculty of Electrical Engineering and Communication, Brno University of Technology, Technická 2848/8, 61600 Brno, the Czech Republic

² Central European Institute of Technology, Purkyňova 656/123, 61200 Brno, the Czech Republic

³ Institute of Physics of Materials, the Czech Academy of Sciences, Žitkova 22, 61662 Brno, the Czech Republic

⁴ Directorate of Research, Development and Innovation Management (DMCDI), Technical University of Cluj-Napoca, Constantin Daicoviciu Street, No. 15, 400020 Cluj-Napoca, Romania

⁵ Department of Ceramics and Polymers, Faculty of Mechanical Engineering, Brno University of Technology, Technická 2896/2, 61600 Brno, the Czech Republic

* Correspondence: stefan_ta@yahoo.com or stefan.talu@auto.utcluj.ro; Tel.: +40-264-401-200; Fax: +40-264-592-055

† Current address: Affiliation 3.

‡ Current address: Affiliation 2.

Abstract: This review summarizes the current trends and developments in the field of polyvinylidene fluoride (PVDF) for use mainly as a nanogenerator. The text covers PVDF from the first steps of solution mixing, through production, to material utilization, demonstration of results, and future perspective. Specific solvents and ratios must be selected when choosing and mixing the solution. It is necessary to set exact parameters during the fabrication and define whether the material will be flexible nanofibers or a solid layer. Based on these selections, the subsequent use of PVDF and its piezoelectric properties are determined. The most common degradation phenomena and how PVDF behaves are described in the paper. This review is therefore intended to provide a basic overview not only for those who plan to start producing PVDF as energy nanogenerators, active filters, or sensors but also for those who are already knowledgeable in the production of this material and want to expand their existing expertise and current overview of the subject.

Keywords: degradation; electrospinning; fabrication; nanofibers; nanogenerator; piezoelectricity; polymer; PVDF; solutions



Citation: Papež, N.; Pisarenko, T.; Ščasnovič, E.; Sobola, D.; Țălu, Ș.; Dallaev, R.; Částková, K.; Sedlák, P. A Brief Introduction and Current State of Polyvinylidene Fluoride as an Energy Harvester. *Coatings* **2022**, *12*, 1429. <https://doi.org/10.3390/coatings12101429>

Academic Editor: Wei Xu

Received: 6 September 2022

Accepted: 22 September 2022

Published: 29 September 2022

Publisher's Note: MDPI stays neutral with regard to jurisdictional claims in published maps and institutional affiliations.



Copyright: © 2022 by the authors. Licensee MDPI, Basel, Switzerland. This article is an open access article distributed under the terms and conditions of the Creative Commons Attribution (CC BY) license (<https://creativecommons.org/licenses/by/4.0/>).

1. Introduction

Nowadays, there are countless synthetically produced polymers with different properties and functions. Organic polyvinylidene fluoride (PVDF) can be classified as one of the most interesting. The reason that has made it so popular is due to its vast range of applications precisely because of its properties [1]. This semicrystalline fluoropolymer has a considerable chemical resistance, high mechanical strength, extensive operating temperature range (the glass transition temperature is $-35\text{ }^{\circ}\text{C}$ and the melting point is $177\text{ }^{\circ}\text{C}$). Moreover, it is biocompatible and highly hydrophobic. It can be argued that similar properties can be achieved with other types of polymers, which is certainly true. For example, polytetrafluoroethylene (PTFE) is regarded as an ideal alternative, but quite expensive [2]. As another similar, fluorinated ethylene propylene (FEP) can be considered, which is suitable for generators in an outdoor environment [3–5]. However, PVDF has one other unique property, and that is the ability to generate a charge, not only using the triboelectric effect but also using piezoelectricity, which is a great advantage over other polymers. Thus, PVDF can rightly be called a nanogenerator. Scientists in many fields are exploring the combination of all these properties and the ability to generate a charge [6–11]. This paper selects a few of the most widely used and interesting ones. In general, these

energy harvesters have taken the name of piezoelectric nanogenerators (PENGs) or triboelectric nanogenerators (TENGs). Although there are many other and not less interesting representatives of both PENGs or TENGs [12], PVDF can also act as a hybrid in both cases [10], and this capability makes it quite distinctive.

First of all, it is necessary to describe PVDF in terms of its chemical structure. The chemical formula is $(C_2H_2F_2)_n$. Its basic building blocks are therefore carbon, hydrogen, and fluorine. These three elements can form several crystalline chain conformations [13]. Conformations are defined by polar and nonpolar phases. Four phases are most commonly found in the literature: α -, β -, γ -, and δ -. Less commonly mentioned is a fifth ϵ -phase [14]. Phases α and ϵ belong to the nonpolar ones. Molecules with antiparallel packing of the dipoles are nonpolar bonds and have no dipole moment [14]. Conversely, polar molecules do not have a full covalent bond, so an imbalance in the electron charge of the molecule is present. The imbalance in the distribution of electrons generates dipoles. The dipoles will try to align themselves when an electric field is provided. The polarity of a molecule affects the attraction between molecular chains. Furthermore, nonpolar polymers are less permeable to water than polar polymers [15]. Thus, it is clear that the polar phases are the most interesting to observe in the case of charge generation. The most associated with charge generation is the β -phase [14]. Furthermore, not neglected is the polar γ -phase, where its polarization effect is weaker. This is because the gauche bond exists in every fourth repeat unit [16]. The often mentioned nonpolar α -phase is usually obtained from the melt by crystallization. The phase conformations of PVDF polymer are illustrated in Figure 1, where their different structures can be clearly seen.

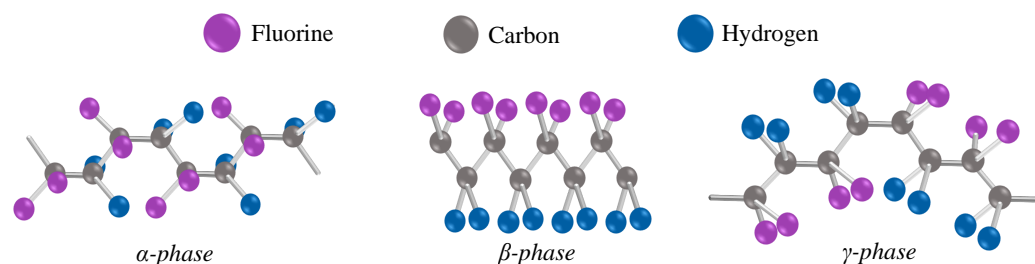


Figure 1. The chain conformation of the most observed phases in PVDF [17]. Because the fluorine atoms in the β -phase are situated on the same side of the molecular chains, which are arranged parallel to one another in a specific direction, with the same dipole orientation and enhanced polarity, the β -phase exhibits spontaneous polarization strength as well as pyro- and piezoelectric properties [18].

Popular methods for phase characteristics are Fourier transform infrared spectroscopy (FTIR), Raman Spectroscopy, X-ray diffraction (XRD), and differential scanning calorimetry (DSC). These methods are discussed later in Section 2.5.

The main effort during production is to increase the β -phase as much as possible. The simplest option is to change the fabrication parameters. The second option is to dope the material with so-called fillers. These also serve, for example, to increase permittivity or hydrophobicity, depending on the application of the material. All of the above issues and more are also discussed in the following sections.

As PVDF is a well-known and used material, it has been the subject of many reviews. Special types of applications or manufacturing are described. A selection of other and recommended papers on a related topic is mentioned in Table 1.

In this paper, the manufacturing and analysis of PVDF polymer is described in a comprehensive Section 2, where the main aspects that should be followed in the production of this material are highlighted. However, once production has been successfully mastered, there are risks that can cause degradation, which Section 3 discusses. As PVDF nanogenerators are currently widespread in many fields, Section 4 maps their current applications. On the contrary, Section 5 pushes the state of the art and goes further, describing new, emerging, and future trends. Finally, all findings presented so far are summarized in the conclusion in Section 6.

Table 1. Selected publications on a similar topic. The chosen studies are mainly complementary to the current paper.

Review Title	Short Description
<ul style="list-style-type: none"> A comprehensive review on fundamental properties and applications of poly(vinylidene fluoride) (PVDF) [19] 	Properties of PVDF and not only its applications as a nanogenerator.
<ul style="list-style-type: none"> Application and modification of poly(vinylidene fluoride) (PVDF) membranes—A review [20] 	PVDF mainly as membranes, their modification and comparison.
<ul style="list-style-type: none"> A brief review on piezoelectric PVDF nanofibers prepared by electrospinning [21] 	A short review focused on electrospinning.
<ul style="list-style-type: none"> Solution blow spinning of polyvinylidene fluoride based fibers for energy harvesting applications: a review [22] 	Alternatives for electrospinning.
<ul style="list-style-type: none"> Progress in piezoelectric nanogenerators based on PVDF composite films [23] 	Special and emerging types of fillers.
<ul style="list-style-type: none"> Electrospun PVDF nanofibers for piezoelectric applications: a review of the influence of electrospinning parameters on the β phase and crystallinity enhancement [24] 	Tuning the β -phase and crystallinity of nanofibers fabricated by electrospinning.
<ul style="list-style-type: none"> Progress in the production and modification of PVDF membranes [25] 	Rich review on membranes, many comparisons.
<ul style="list-style-type: none"> Recent advances in the preparation of PVDF-based piezoelectric materials [26] 	Fabrication, preparation, and β -phase formation of PVDF and its copolymers.

2. Materials and Methods

How to prepare the right solution (Section 2.1), how to choose (Section 2.2) and how to make (Section 2.3) fibers or layers from this solution, how to enhance the obtained material (Section 2.4), and how and what to measure (Section 2.5) are covered in this section. Various recommendations, known problems, or even possible interesting facts that many scientists over the last years have discovered can be found here.

2.1. Solution Preparation

For the formation of the material, the preparation of the solution precedes. The PVDF must be processed into a liquid form using a solvent, and if necessary, a specific filler must be added in the process. As PVDF has a relatively high toxic resistance, it is not easy to dissolve, and only small amounts of polar solvents need to be used. The standard solvents used are dimethyl sulfoxide (DMSO), dimethyl formamide (DMF), dimethyl acetamide (DMAc), or *N*-methyl pyrrolidone (NMP). These solvents are often combined with acetone (Ac) with various ratios. The addition of smaller amounts of acetone contributes to the volatilization of the solvent and an increase in the β -phase [24]. Acetone causes a faster evaporation of the solvent. There are also several papers experimenting with different solvent ratios [27] but DMSO/Ac with a 7:3 ratio is quite commonly used [6,28–30]. The amount of acetone is also reported with the ratio of 6:4 for DMF/Ac, DMSO/Ac, and NMP/Ac [31]. Different ratios have also been shown to affect the morphology of nanofibers [32]. Furthermore, the choice depends on the PVDF concentration. This is given in the range of 10 to 25 wt% [24,31,33]; the choice will of course affect the viscosity of the solution. Subsequently, essential parameters such as chain conformations are also affected. The optimum selection for a high β -phase is 20 wt% PVDF, then with a higher concentration the β -phase decreases. Lastly, molecular weight is also important. It also influences the viscosity of the resulting solution. Molecular weights of 70.000, 180.000, 275.000, 534.000, and 777.000 g/mol have already been used. The most currently used value for electrospinning is 275.000 g/mol [33–39]. After selecting the appropriate type of PVDF

and solvent, these substances are mixed. A standard stirrer at 40 to 80 °C is used, and the mixing time should be at least 4 h. However, many authors choose 24 h with known solvents such as DMSO, NMP, or DMF [40].

Nevertheless, it is essential to keep in mind that the parameters chosen in this way may affect the β -phase and other chain conformations. However, what matters most is the subsequent method of production and the capabilities of the apparatus. In particular, using nanofiber fabrication by the electrospinning method can lead to needle clogging during its use. When preparing the solution, it is advisable to take into account the way in which the resulting piezoelectric polymer will be processed.

Other lesser-known solvents for PVDF are as follows: acetyl triethyl citrate (ATEC), γ -butyrolactone (GBL), cyclohexanone (CHO), cyclopentanone (CPO), dibutyl phthalate (DBP), dibutyl sebacate (DBS), diethyl carbonate (DEC), diethyl phthalate (DEP), dihydrolevoglucosenone (Cyrene), 1,4-dioxane, 3-heptanone, hexamethyl phosphoramide (HMPA), 3-hexanone, methyl ethyl ketone (MEK), 3-octanone, Rhodiasolv PolarCleansa, 3-pentanone, propylene carbonate (PC), tetrahydrofuran (THF), tetramethylurea (TMU), triacetin, triethyl citrate (TEC), triethyl phosphate (TEP), trimethyl phosphate (TMP), and *N,N'*-tetrabutylsucciniamide (TBSA) [41–43].

2.2. Fibers or Solid Layers?

Where and how the material will be used also determines whether the PVDF will be in the form of nanofibers or solid layers. Both have advantages and disadvantages, and scientists are experimenting with them [18]. For obvious reasons, a significantly stronger piezo effect, and not only that, can be expected with solid layers—films. Here, one must consider the reduced flexibility or the impossibility of using the material as a filter (often also for the utilization of photocatalysis [44]), which is not the case with nanofibers. However, the characterization of nanofibers is much more challenging than for solid layers. Indeed, the fiber mat is an inhomogeneous material where the individual fibers are chaotically distributed. While the arrangement of the fibers can be controlled (e.g., by the rotation of the collector cylinder during electrospinning), it is not such that it can be accurately quantified and has not yet been described mathematically. The fiber mat is filled with air, which affects every measurement. The interpretation of the results is then much more complex, for example, in any spectroscopic measurement due to the uneven structure or in electrical measurements, such as permittivity, where the air inside the fiber mat is partly measured. Therefore, these are negative properties that must be taken into account when choosing nanofibers.

2.3. Material Fabrication

Electroactive PVDF can be formed in two variants—fibers or layers. As outlined in previous sections, the choice of the form of this material depends mainly on the area of use. Thus, if there are high requirements for flexibility, breathability, or even elasticity, it is better to define the form of the fibers. In this case, such a nanogenerator finds perfect use in the field of tissue engineering [45], smart textiles [46], or as an active filter [47]. Otherwise, layers or rather thinner films can be used, for example, as a pressure sensor [48,49].

Currently, the most widely used methods for producing PVDF nanogenerators, sensors, membranes, and other electrical-signal-generating products include spin-coating—for thin films [23,50], and electrospinning—for fibers. Electrospinning in the field of nanogenerators is relatively predominant [24,51–54]. Other lesser-known methods include electrospraying—a layer in the form of nanoparticles [55,56], or the Langmuir–Blodgett method—a layer formed by chemical deposition [57,58]. Using the method of electrospinning is quite extensive and is divided into many subcategories of how electrospinning can be performed. Notwithstanding, the basic principle is the same—in a high voltage system, a liquid solution in the form of a fiber is drawn by an electric force between the emitter and the collector. Due to the electric field, the so-called Taylor cone forms on the emitter, which acts as the liquid source. At the tip of this cone, the fiber is pulled towards whipping the collector (Figure 2). The result is a nanofiber structure.

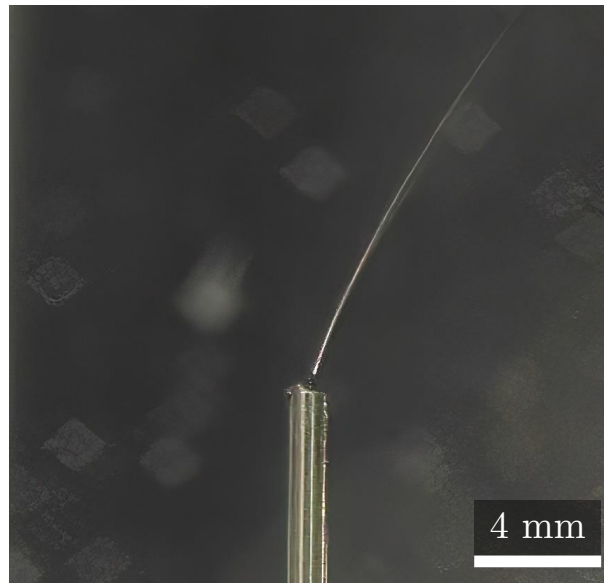


Figure 2. Drawing of a fiber from a forming Taylor cone at the tip of the emitter, in this case, a needle. The fiber is attracted towards the collector, which is no longer captured in this image. The material is 20% PVDF. The heated solution is still liquid in the emitter but during the whipping of the collector and fiber formation the solvent dries, and the PVDF solidifies [17].

The most well-known electrospinning method is when the needle is placed as the emitter, through which the solution flows towards the collector, which is in the form of a rotating cylinder (Figure 3). Researchers like this method mainly because they can very carefully control every parameter of production of literally every fiber on the resulting fiber mat. The thickness of the fibers and their shape, tension, or evaporation time can be controlled, for example, the distance between the emitter and collector, the high voltage value between them, cylinder rotation speed, needle diameter, solution flow rate, or air temperature or atmosphere in a chamber where the fiber is formed. The following Table 2 lists the most common problems that can occur with single-needle electrospinning on the rotating collector [30,59,60].

Table 2. The most common electrospinning problems in which PVDF nanofiber imperfections occur [30,59,60].

Problem	Cause
Fiber bonding	Short emitter–collector distance
Formation of droplets in fibers	High dosing rate (emitter flow)
	High emitter–collector voltage
Nonformation of droplets in fibers	High viscosity
Chaotically oriented fibers, thick fibers	Low emitter–collector voltage
	Low collector cylinder speed
	Higher molecular weight
Spinning outside the cylinder	Low emitter–collector voltage
	High collector cylinder speed
Low fiber tension	Solution without ions/salts (small number of charges)

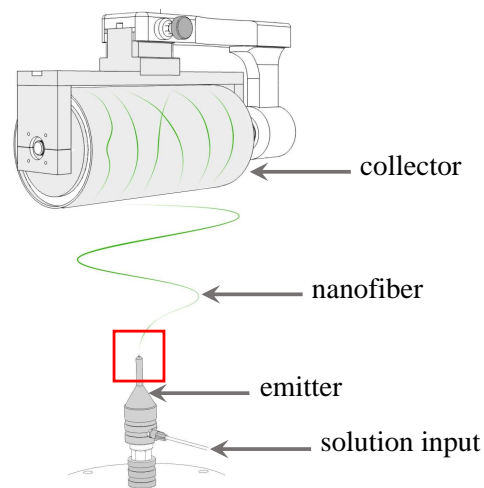


Figure 3. Illustration of the method of electrospinning in the form of a single needle acting as an emitter and a rotating cylinder acting as a collector, on which the nanofiber is gradually wound, and as a result it then creates a kind of fabric that can be used as the basis of a simple nanogenerator [17]. The red square highlights the emitter—the needle with the solution changing to a fiber, which was also described in Figure 2.

In this way, the specific parameters of the fiber can be achieved relatively accurately, and the β -phase of the resulting fiber can be successfully tuned [24]. The labeling as “nanofibers” can rightly be used for the size of such fibers, as their thickness can range from microns to tens of nanometers [61]. In some cases, it is even possible to create structures in the order of nanometer units. Černohorský et al. in Figure 4 demonstrated that these structures resembling a cobweb were formed in the combination of PVDF and nylon-6 (PA6) [61].

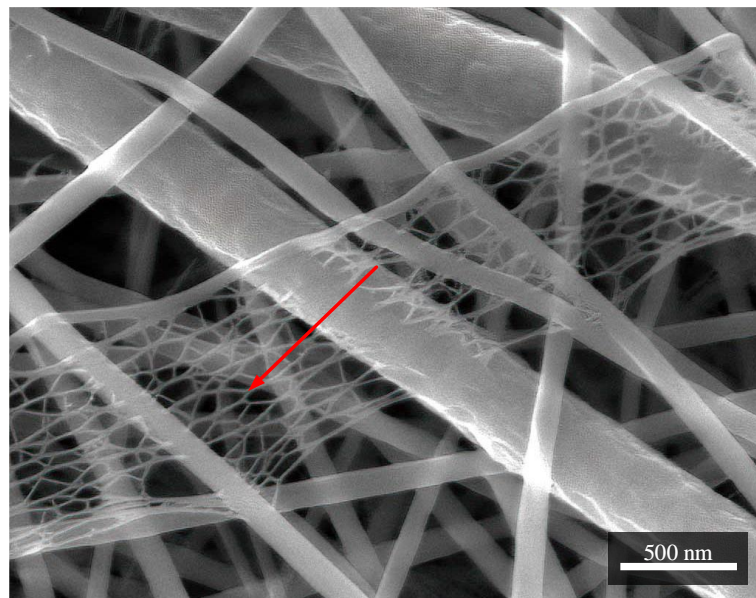


Figure 4. A structure of porous character resembling a cobweb. This structure was observed in combination with nylon-6 (PA6) [61]. The structures of smaller nanofibers within tens of nanometers are indicated by the arrow.

However, this precise production control based on a single drawn fiber is, of course, redeemed by the production time when the fiber is wound on the cylinder. This can be solved relatively easily by replacing one needle with two or more but at the cost of less control over the process. Furthermore, as already mentioned, electrospinning exists in many variants. Thus, for example, a coaxial needle can be used instead of a single needle,

where two types of solutions flow through the needle and where the fiber core can thus be of a different type than its shell. This type of nanofibers is also called core-shell nanofibers. It is also a relatively popular method [62–64]. Instead of the coaxial needle, two different needles with different solutions or several more needles can be used. The so-called metal rod can also be used instead of needles. However, compared to Figure 3, the emitter serves as the metal rod from which liquid is released, placed from the top, and the collector from the bottom. If the electrospay method is considered, it is necessary to use the appropriate part (instead of the needle) as the emitter. The type of collector can also be changed, where a static plate can be used instead of the rotating cylinder on which the fiber would be applied. Nevertheless, the rotating cylinder can also serve as the emitter when it is partially immersed in the solution and constantly wets into it during rotation and thus “brings” the solution to the collector, where the material is again drawn in the form of fibers. No higher control can be expected here when drawing the fibers. It is also worth noting that a solution is not always used in electrospinning. With the required aperture, direct melting of the material can also occur at the cost of a much higher viscosity [65].

2.4. Tuning and Improving the Properties

Although PVDF can be considered a very successful and popular material, perhaps also because of this, scientists are constantly trying to improve its properties. There are a large number of articles in the databases not only about how to improve its β -phase, which is usually the primary goal but also about how to improve other properties, such as hydrophobicity, tensile strength, etc., [66–72].

The first option is to adjust the production parameters [73]. For example, several research groups have shown that the β -phase for the fibrous PVDF structure can rise by increasing the speed of the collector cylinder. Higher collector cylinder speeds can also cause different material flexibility. In this case, the arrangement of the fibers in the overall fiber mat is different. At low speeds of around 300 rpm, the fibers are much more chaotically distributed. At high speeds, such as 2000 rpm, the fibers are again much more aligned, i.e., made tensile and thus with smaller diameters. That is why electrospinning with the needle and the rotating cylinder is so much used [17,30,51,61,74].

The second option is doping, mixing, and adding additional material. The result is a new composite. It could be, for example, the previously mentioned nylon (PA6), which can be spun in parallel with PVDF, and which can be used to control hydrophobicity, stress, and the magnitude of the triboelectric effect etc. [6,51]. The core-shell is often used, i.e., a combination of two solutions using a coaxial needle [64,75–77]. The variation of solutions to PVDF is relatively large, so it cannot yet be said with certainty that one composite predominates more than another.

Another option is to use fillers, which are various powders mixed with a solution. However, it is necessary to pay much more attention to the affinity of the material and thus check its mutual compatibility [78–80]. For example, there are efforts to improve ferroelectric and magnetic properties with BiFeO_3 [81–84], or also with the relatively popular BaTiO_3 to increase the β -phase [78,85–91]. Other authors use ZnO to improve output voltage and improve crystalline structure [92,93]. There is also a rich use of PZT ceramics to increase piezoelectric properties [94], which can also be used as a smart air filter [95]. Almost all of these methods use electrospinning. Of course, this selection does not cover (nor is it intended to) the very broad combination of materials that are used with PVDF. However, the possibilities mentioned are ones of the most common.

2.5. Characterization and Electrical Measurement Methods

This part of the section describes the most widespread methods of characterization, material composition, and electrical properties of PVDF, especially nanofibers. The most investigated parameter of this material is usually its phase conformation, which is associated with the piezoelectric effect. The large part of the work is then focused mainly on studying the β -phase. All these results are based on the used spinning methods, specific production parameters, fillers, but also on the specific type of (commercial) PVDF [14,96–101]. For

spectroscopic methods studying fibers, the characterization of fibers can be considered relatively complex. The reason is simple, namely, the inhomogeneous structure of the sample surface, so it can be assumed that these methods will be more accurate for solid PVDF layers [17,74,102].

For ease of reference, Table 3 below summarizes the most commonly used methods for PVDF analysis with a brief description of each technique.

Table 3. The most used methods for the study of PVDF nanogenerators.

Measurement Method	Short Description
Scanning electron microscopy (Section 2.5.1)	Structure, shape, thickness, cross section
Fourier transform infrared spectroscopy (Section 2.5.2)	Determination of the phase conformations
Raman spectroscopy (Section 2.5.3)	Similar to FTIR, sample fingerprint analysis
X-ray photoelectron spectroscopy (Section 2.5.4)	Elemental composition
X-ray diffraction (Section 2.5.5)	Structure of a crystal, phase conformations
Atomic/piezoresponse force microscopy (Section 2.5.6)	Fiber diameter, piezoresponse
Permittivity and dielectric properties (Section 2.5.7)	Dielectric constant ϵ_r
Piezoelectric coefficient (Section 2.5.8)	Piezoelectric coefficient d
Wettability (Section 2.5.9)	Contact angle
Surface area analysis (Section 2.5.10)	Gas adsorption
Thermogravimetric analysis (Section 2.5.11)	Weight percentage composition, thermal properties
Differential scanning calorimetry (Section 2.5.12)	Crystallinity
Mechanical properties (Section 2.5.13)	Tensile stress, Young's modulus, and tensile strain

2.5.1. Scanning Electron Microscopy (SEM)

It is used mainly for studying the structure of nanofibers. There are several reasons for its use. One of the main reasons is to examine the condition of the fiber—its shape, thickness, and defects [32,68]. It is also possible to perform statistical calculations [32,88,102–104] and observe the attachment of various fillers. In the case of experiments with production parameters that affect the physical properties of fibers, SEM is a necessary method. This method may also include an FIB (Figure 5) [17] for examining the fiber cross section or an EDS for an elemental analysis [105].

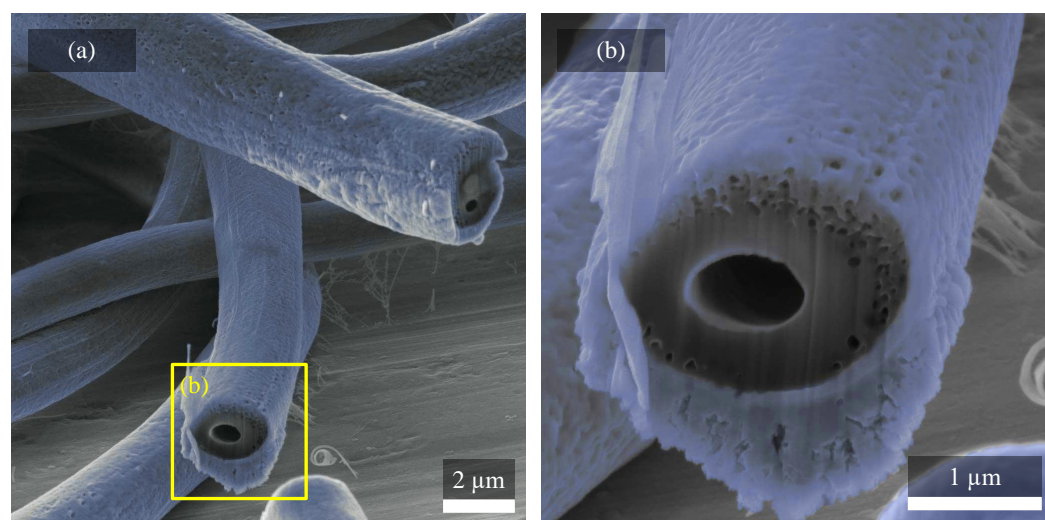


Figure 5. Example of PVDF nanofibers that have been cut using FIB. Several interesting aspects can be seen in (a). In the fiber cut at the upper part, it can be seen that its structure is not perfectly oval. Both cut fibers appear hollow in some parts, or it may also be an air bubble. On closer examination in (b), it can be seen that particularly in the surface region, the fibers are quite porous. Since PVDF is the polymer, it has been coated to prevent charging of fibers, as indicated by the color highlighting [17].

2.5.2. Fourier Transform Infrared Spectroscopy (FTIR)

A relatively popular and frequently used method just after SEM characterization is FTIR, where its use for PVDF investigation is in the order of hundreds of papers [106]. It is used to accurately determine the phase conformations in the sample. The exact proportion of the β -phase can thus be calculated quite accurately [17]. The determination of PVDF phases is not identical among all authors, but there are also exclusive peaks or even dual peaks (mainly β - γ) (Table 4). In some cases, the attenuated total reflection system ATR with FTIR is also used to determine the functional groups and bonds (for example, with hydrogen) [107]. The group CH_2 bending vibration occurs at 1402 cm^{-1} , the CF_2 bending vibration at 508 cm^{-1} and 473 cm^{-1} , and the stretching band at 1180 cm^{-1} [108–110]. There is also a shift of about 2 cm^{-1} in some articles [106].

Table 4. List of the most commonly identified values for α -, β -, and γ -phases in FTIR absorption spectrum. The last line also lists the values of the so-called dual peaks, as they are denoted by some authors [97,106,111].

Spectral Area	Value
α -phase peak	410, 489, 532, 614, 763, 795, 854, 975, 1149, 1209, 1383, and 1423 cm^{-1}
β -phase peak	445, 473, and 1275 cm^{-1}
γ -phase peak	431, 482, 811, and 1234 cm^{-1}
Dual β - γ peak *	510, 840, and 881 cm^{-1}

* Some authors consider these dual peaks to be purely β -phase, others purely γ -phase, the largest divergence can be considered at 840 cm^{-1} .

2.5.3. Raman Spectroscopy

Raman spectroscopy is also used for a precise phase and sample fingerprint analysis, like FTIR, and thus considered to be a complementary or alternative method due to its similar characteristics. The reasons for the use of both methods may also be as a result of the aforementioned inhomogeneity of the nanofiber sample surface, where the outcomes from the characterizations may correlate each other. Although we want to display the same phase, it can differ between FTIR and Raman spectroscopy, as Raman spectroscopy can show different rotations, bending, and stretching of molecules. It also depends on the light source used for Raman spectroscopy and device sensitivity on the lower wavelengths. The fraction crystallinity of each phase can be calculated from Raman as well as from the FTIR [112]. Furthermore, here again, several less intense peaks can be found in the spectrum, which have been adequately described [74,102,113,114]. Typical wavenumbers for the crystalline phases from Raman spectroscopy are: the α -phase occurring at 794 and 874 cm^{-1} , the β -phase or the β - γ combination found at 839 cm^{-1} , and the γ -phase found at 812 cm^{-1} [115]. Since, the polymer is investigated by Raman spectroscopy, it is not recommended to set the laser power higher than in mW units.

2.5.4. X-ray Photoelectron Spectroscopy (XPS)

Because XPS tracks the elemental composition on the surface of a sample, it is not as commonly used as further spectroscopic and other methods for determining phase structure. However, it is relatively important for accurate monitoring material changes, for example, when using different solvents or fillers. The most commonly observed regions for PVDF are carbon C1s, fluorine F1s, their bonds, and possibly hydrogen H bonding [116]. For example, the peaks at 286 eV originated from the $-\text{CH}_2-$, and the one at 290 eV originated from the $-\text{CF}_2-$ components, the one at 288 eV originated from the $-\text{CH}-$, and the one at 293 eV corresponds to $-\text{CF}_3-$ groups. Some bonds cannot be easily detected without fitting. Hydrogen itself is undetectable by XPS.

2.5.5. X-ray Diffraction (XRD)

It is a crystallographic method used to analyze the phase structure of a sample. It is standardly expressed as intensity vs. 2θ . All PVDF phases here have specific values in units of degrees. The characteristic patterns of PVDF are mainly between 14 and 26° [117]. The β -phase has a characteristic value of 20.26° . Saha et al. states its value of 20.4° [118], Moazeni et al. reports a β -phase of $2\theta = 20.6^\circ$ (200/110) [117], Chethan et al. provides $2\theta = 20.8^\circ$ (110/200) [119]; the α -phase peaks occur at 17.7° , 18.3° , and 19.9° ; the γ -phase peaks are 18.5° , 19.2° , and 20° [14,120]. It is obvious that, for example, 20° for the γ -phase can be easily mistaken for the β -phase and vice versa.

2.5.6. Atomic Force Microscopy (AFM) and Piezoresponse Force Microscopy (PFM)

Using AFM, it is also possible to measure the piezoresponse of the sample, i.e., its ferro- and piezoelectric domain, specifically when using the PFM mode. In most cases, this is a very precise examination of only one fiber with a diameter of 100 nm to 3000 nm [18,24,121–123], where the authors prove the properties of a particular sample (Figure 6) [120,124].

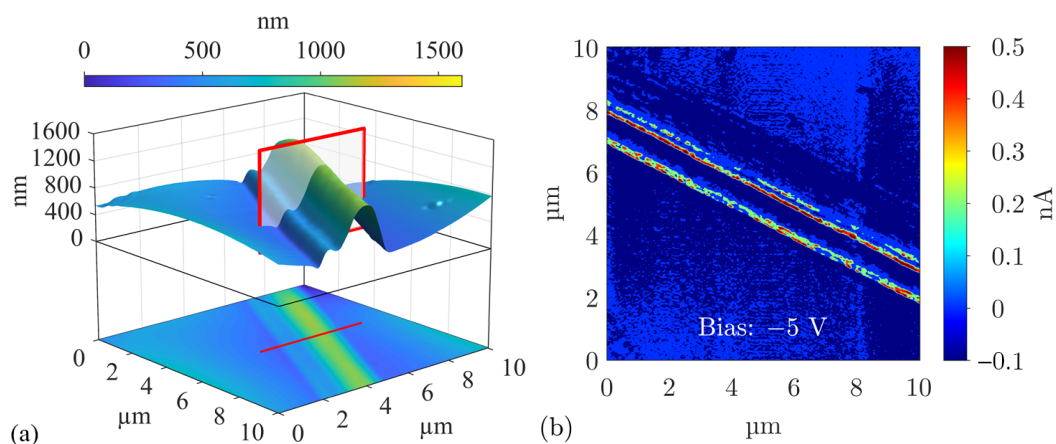


Figure 6. (a) Fiber similar in shape to the one that was acquired by SEM and mentioned in Figure 5a. The same fiber is also measured using the (b) PFM method, where the authors confirm the different orientation of the domains with a bias of -5 V [17].

2.5.7. Permittivity and Other Dielectric Properties

Permittivity is an important electrical property that affects charge generation. For polymers, permittivity is limited by a low intrinsic dielectric constant ϵ_{eff} . In nanofiber PVDF, it can be increased mainly by adding ceramic fillers or by forming a composite [90]. In this case, solid layers have a higher permittivity for obvious reasons (Section 2.2). When measuring a nanofibrous material, the sample is largely filled with air, which complicates the measurement, makes it harder to determine the specific thickness of the material (which must be known when measuring permittivity), and generally reduces the resulting value. It is not entirely surprising that the resulting real part of the permittivity is close to the value of the relative permittivity of the air. The dielectric constant ϵ_r or ϵ' of a normal undoped pure sample at 100 Hz is around 1.5 – 3 [61,125], and for most PVDF samples is not higher than 10 . If no characteristic is given, the values at 1 kHz should also be added. In addition, the loss coefficient $\tan \delta$ or the imaginary component ϵ'' is usually stated.

High dielectric properties are expected to result in increased energy storage density. Given the constant miniaturization, this capability of the material is also highly demanded and desirable. Table 5 shows selected research that aims to maximize energy storage density. It is apparent from the results that polymers with several layers achieve the highest values.

Table 5. Concise demonstration of several selected PVDF composites having high dielectric properties.

Utilized Composite	Achieved Energy Storage Density
6-fold P&F PVDF films [126]	39.80 J/cm ² at 880 kV/mm
BaTiO ₃ /PVDF layers [127]	20.70 J/cm ² at 690 kV/mm
BiFeO ₃ TiO ₂ -PVDF/PMMA [128]	19.30 J/cm ² at 549 kV/mm
BN/PVDF/BN [129]	19.26 J/cm ² at 465 kV/mm
Three-layer PVDF [130]	11.00 J/cm ² at 440 kV/mm
Pure PVDF [127]	9.30 J/cm ² at 500 kV/mm
3 wt% BZT-BCT NFs/PVDF [131]	7.86 J/cm ² at 310 kV/mm
0.1 wt% graphene/P(VDF-TrFE-CFE) [132]	7.00 J/cm ² at 300 kV/mm
BaTiO ₃ -CoFe ₂ O ₄ /PVDF [133]	5.60 J/cm ² at 263 kV/mm
1.25 wt% Ba(Zr,Ti)O ₃ /P(VDF-TrFE-CFE) [134]	2.80 J/cm ² at 75 kV/mm

2.5.8. Piezoelectric Coefficient

Although the high β -phase is a prerequisite for a high piezoelectric effect, some experiments are combined with the measurement of the piezoelectric coefficient [124]. The piezoelectric coefficient d , more precisely piezoelectric charge coefficient or piezoelectric strain coefficient, belongs to the group of piezoelectric constants, which also includes piezoelectric voltage coefficient g , piezoelectric stress coefficient e , and piezoelectric stiffness coefficient h .

The piezoelectric coefficient d_{ij} is defined by two subscripts i and j and is most often given in pC/N units. Subscripts i and j are expressed by numbers that represent the designation of the axes and the directions of deformation. Subscript i shows the direction of polarization, and subscript j shows the direction of the applied stress. The compression mode, as the d_{33} coefficient is otherwise called [135], is one of the most frequently observed piezoelectric characteristics in PVDF [136–140]. It indicates that mechanical deformation occurs in the same direction as the polarization. Another of the common piezoelectric coefficients is d_{31} or transverse mode, where mechanical stress is applied at right angles to the polarization axis. The following empirical relationship holds between d_{33} and d_{31} [141]:

$$d_{33} \approx -2.5 \cdot d_{31} \quad (1)$$

The results from the measurements vary widely depending on the application of the fibers/layers. Standard results are usually in tens of pC/N units. When using ceramics, values in the hundreds of pC/N can be achieved. In the case of other electrical characteristics, for example, the voltage response [142,143] or hysteresis loop [14] is widely measured.

2.5.9. Wettability

The hydrophobicity and hydrophilicity of PVDF are another of the relatively frequently investigated properties [144]. These properties may be important, for example, for active filters, membranes [66,67], or textiles [145,146]. It has been shown that with a higher collector cylinder speed during electrospinning, these properties can be controlled (Figure 7) [17]. Various collector speeds give the sample structure a different morphology, and as the collector speed increases, the fibers become more aligned. It is generally known that PVDF is a hydrophobic material, and researchers are trying to modify it to higher values up to superhydrophobic properties, with a contact angle $>150^\circ$ [68,147].

2.5.10. Brunauer–Emmett–Teller (BET) Surface Area Analysis

It is a standardized technique (ISO 9277) for determining surface areas that uses a measurement of a physisorption of a gas. Most often gas adsorption in units of area per mass of sample (m²/g) is mentioned, but it may also be given as area per volume (m²/cm³). It is performed using the adsorption of nitrogen (most often) at 77 K, argon at 87 K, krypton at 77 K, carbon dioxide at 0 °C or 25 °C, and water at 20 °C. The specific results for PVDF with fillers vary. Rosman et al. stated [148] that for pure PVDF nanofibers, the specific surface was revealed to be about 3.76 m²/g, and increased with the addition of ZnO up to 6.61 m²/g.

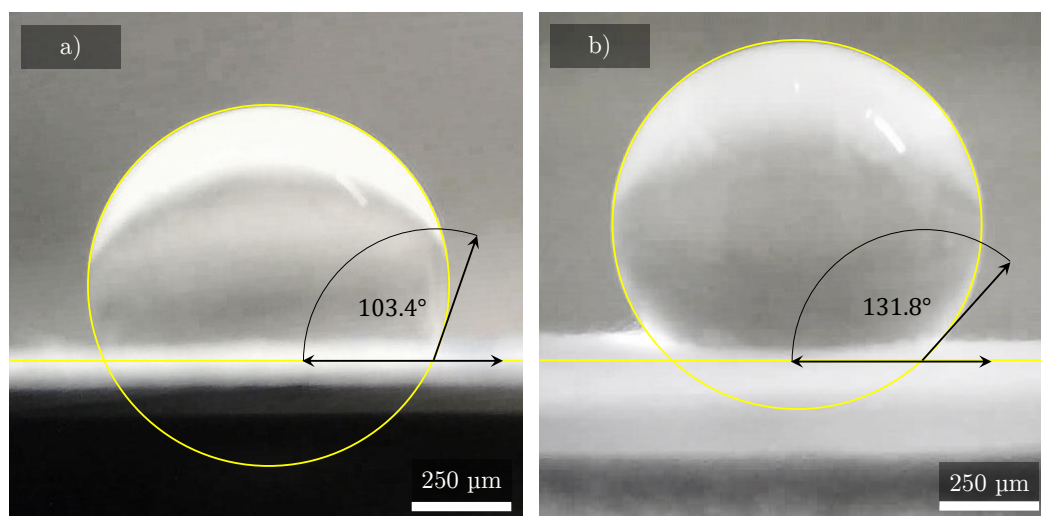


Figure 7. Captured images shows the hydrophobicity of the same type of PVDF without any fillers, produced by the method of electrospinning with different rotation of the collector cylinder. The figure shows the contact angle of a 3 μL distilled water droplet on the PVDF nanofiber mat. Sample (a) was made with the rotation of 300 rpm, and sample (b) with the rotation of 2000 rpm. The difference in contact angle is almost 30° [17].

Yardimci et al. in their work reported [149] that PAN/PVDF nanofibers with 5 wt% AgNO_3 was 22.09 m^2/g , with 10 wt% AgNO_3 was 11.58 m^2/g , and with 20 wt% AgNO_3 , it was 5.97 m^2/g . Thus, the opposite trend to that of Rosman et al. with a ZnO filler [148].

Cvek et al. [150] in their research using combined PVDF/PVDF-TrFE blends loaded with BaTiO_3 obtained a value of 17 m^2/g .

2.5.11. Thermogravimetric Analysis (TGA)

By so-called thermographs, PVDF is characterized by the weight percentage composition, thermal properties, and stability of the sample [151]. By default, it is compared with doped samples to determine the weight loss of the doped sample. For pure PVDF, degradation has been measured by most authors at a temperature around 430 °C [69,152–155].

2.5.12. Differential Scanning Calorimetry (DSC)

The crystallinity of PVDF is usually investigated with DSC. The heat which is associated with the fusion of the polymer is quantified [69]. The melting point T_m , heat of fusion ΔH_f , and of course crystalline phases X_C [124,156–158] are most often mentioned. In the case of the original PVDF, the crystallinity X_C value can be up to 80% [159], but this is a relatively high value and values of around 50% most often occur in scientific studies [17,30,89,111,151].

2.5.13. Mechanical Properties

Some works also test the mechanical properties of PVDF. Usually, tensile stress (MPa), Young's modulus (MPa), and tensile strain (%) are tested [103]. It is generally known that the PVDF structure contains pores that can affect mechanical properties [147]. PVDF can be reinforced, for example, in combination with nylon [61] or silver [69].

An important parameter for specifying the mechanical properties of fibers is the fiber volume fraction V_f [160], which according to standard ASTM D2584 is defined as

$$V_f = \frac{\rho_m \cdot w_f}{\rho_m \cdot w_f + \rho_f \cdot w_m}, \quad (2)$$

where ρ_m is the density of the matrix, w_f is the weight of the fibers, ρ_f is the density of the fibers, and w_m is the weight of the matrix. Nevertheless, the mentioned fiber volume can change, for example, due to the moisture, which swells the fibers and changes their weight.

This difference can entirely change the mechanical properties of the fiber. If the actual fiber weight (including moisture content) is denoted as w_{fc} , then

$$w_{fc} = w_f(1 - w_c), \quad (3)$$

where w_c is the weight of the water content. Similarly, the density of fibers ρ_f should be modified to the density of the fibers with moisture content ρ_{fc} :

$$\rho_{fc} = \frac{1 + MC}{\frac{1}{\rho_{f0}} + MC}, \quad (4)$$

where MC is the moisture content and ρ_{f0} is the density of the dry fibers. With this assumption, the modified equation of the fiber volume fraction (including moisture content) V_{fc} is

$$V_{fc} = \frac{\rho_m \cdot w_{fc}}{\rho_m \cdot w_{fc} + \rho_{fc} \cdot w_m}. \quad (5)$$

3. Material Reactions and Degradation

As already mentioned, PVDF is a nonreactive polymer and has a high toxic resistance. Its resistance to degradation can be considered higher compared to other polymers [161]. Changes occur mainly with higher temperatures and standardly may be combinations of two or more effects (mechanical properties, crystallinity, color, etc.) [162]. It is commonly able to resist basic solutions, chlorine solution, alcohols, several acids, halogens, and aliphatic or aromatic compounds [19]. PVDF weakens when various alkaline solutions are used [163,164]. Lactic acid $C_3H_6O_3$, nitric acid HNO_3 , sulfuric acid H_2SO_4 , and tetrahydrofuran C_4H_8O are mentioned as having little resistance to acids. Its color may change from pure white to yellow, and during the dehydrochlorination process (loss of hydro fluoride units from the polymer chain), it may darken to black [165]. Furthermore, less resistant are glucose and wine vinegar, which is essentially a concentrate of acetic acid. When exposed to higher temperatures, the damage caused by these substances increases.

Regarding thermal degradation, temperature can affect charge generation mainly because of the weakening of mechanical properties at very low temperatures, i.e., the glass transition temperature of $-35^\circ C$, when the material hardens and becomes more brittle. Below this critical value, the material may degenerate as it loses its elasticity and flexibility, which naturally limits the development of piezoelectric phenomena. This temperature is relatively low compared to commonly known polymers. For example, PTFE has $T_g = 115^\circ C$. On the other hand, at the melting temperature of $177^\circ C$, the crystallization process is affected. For PTFE, $T_m = 327^\circ C$. Exceeding any of these threshold temperatures can lead to a different phase transition of the material, which is addressed, for example, by the previously mentioned DSC [166]. Despite all the mentioned drawbacks, PVDF is very stable within these values and it is often called a thermoplastic polymer. The temperatures mentioned may vary slightly in units of degrees depending on the manufacturer of the commercial polymer type.

For PVDF, which has flexible fibers, the critical issue is mechanical strength which is, of course, very different from solid layers. In fact, a good tensile strength is required for a piezoelectric generator. If the nanofibers do not have additional support, they can be damaged more quickly. Microcracks and point defects can already occur with imperfect fabrication, which can be, for example, a contamination of the microparticles. However, it can still be argued that cracks may not be spread throughout the material in the case of single fibers as opposed to solid layers. The tensile strength, elongation at break, and Young's modulus of the PVDF fiber were measured by Hasim, Liu, and Li [167] in sodium hydroxide NaOH solutions. The results in degradation changes were classified as significant. Here again, the increased temperature also accelerated the aging of the samples.

4. Utilization in Real Applications

Although PVDF can be used as a nanogenerator of energy, it is a relatively broad concept. Therefore, it is appropriate to mention several interesting works that are exper-

imentally devoted to specific applications. Hence, this section does not primarily serve to describe the various fillers and other composite combinations that can improve PVDF properties (which have already been mentioned in Section 2.4), but to describe the direct applications of PVDF itself.

A widespread and intended use of PVDF as a nanofabric is directly for the human body. There can be several uses. The simplest uses can be as a wearable shirt, generating charge when walking and moving [168], during inhaling and exhaling [169], or blood flow [170–172], or as gloves [173]. It can also serve as a shoe insole [49,174–176], or while typing on the keyboard [177]. For these applications, PVDF can operate just as a common sensor (safety monitoring, medical diagnostics), or as a nanogenerator depending on its performance [40,178]. In these cases, the connection to the IoT is also assumed [179]. In addition to such practical uses, PVDF can also be used purely as a green energy harvester, for example, for wind energy harvesting [3,5,180], or for energy harvesting from ocean waves and applications [181,182].

Among the less common but emerging uses may include the use of PVDF as scaffolds in tissue engineering due to its biocompatibility. For example, for osteoblasts (bone cells), where their electromechanical stimulation can accelerate cell spreading [183–185]. For solar cells, PVDF can serve as an enhancer of the crystallinity of currently very popular perovskites [186], when there are already attempts to create a hybrid inducing the piezophototronic effect [187]. Another unique use of the PVDF nanogenerator also appears to be energy harvesting from sound waves [188,189].

5. Future Perspectives

The implementation of clean PVDF fibers or layers themselves as an energy generator seems to be an inexpensive and easy way, but the current trend is to use PVDF mainly as a composite, doped with fillers, for this sector (discussed in Section 2.4). Most databases are oversaturated with papers on experiments with new PVDF composites and combinations as energy generators; and the knowledge on clean PVDF polymer material itself is rather repetitive.

Another interesting point is the continuing and ongoing growth of attention on the topic of wearables. This is understandable and desirable with respect to the forthcoming miniaturization and the fact that PVDF is a mechanically tough material that is flexible in both fiber and film form [168,190,191].

A relatively popular type of energy harvesting in recent years is PVDF as a thermoelectric generator (TEG) [192–196]. That means generating an electrical voltage due to an applied temperature gradient. The Seebeck effect on which TEGs are based of course is not a new concept, but in combination with PVDF, these experiments are emerging, and given their increasing number, their subsequent evolution can still be expected. Similarly, as the β -phase determines the piezoelectric coefficient, it has also been reported to be more thermodynamically favorable [197], and therefore PVDF also becomes a candidate for TEG [198]. It most often acts as a composite together with other materials [199–202], although generally as a film. Fibers such as TEG alone do not appear much in scientific papers yet, which can be concluded due to the expectation of low effectiveness. The use of TEG, especially in a flexible form, is also applied as mentioned above in wearable materials such as body heat harvesting [203–206]. Kumar, Singh, and Khare [207] even used this PVDF generator as a hybrid TEG/PENG, where a PVDF film was encapsulated with TEG.

The hybridization of PVDF and the use of a combination of different possible energy sources at the same time seems to be a very efficient and modern approach, not only for green energy harvesting [44,208]. However, their production is more complex. The most common is the combination of piezo- and triboelectric phenomena, which currently consist of, for example, the already mentioned perovskite structures and PVDF, and which can be considered as a prospective topic [209–212].

6. Conclusions

As a highlight of this review, it can be concluded that it guides the reader from the very beginning of the PVDF nanogenerator design to its final form based on current trends. The review was also written in such a way that its contents can be used by scientists who have not had much experience with PVDF before. On the other hand, for those who already have this knowledge, it may broaden their horizons in the case of new designs and solutions.

It can be summarized from the current research that the scope of PVDF nanofibers is extensive, and their combination potential is considerable. New ways of improving the fibers or layers and where to apply them are constantly evolving. According to the ScienceDirect database, the number of publications on PVDF nanogenerators has been increasing rapidly in recent years, and currently, their total number is already in the thousands. Their significant increase can be seen especially in areas such as material science and energy in the last five years. The most common topics are the aforesaid variations, mixtures, and tuning of nanofibers.

Electrospinning, which can be used to create nanofibrous structures, can be quite reliably identified as the leading fabrication method. However, despite the flexible advantage of PVDF, these structures lose out quite understandably in the areas of charge generation and permittivity. Nonetheless, this is often compensated by the mentioned tuning and doping.

The most popular characterization methods can be considered SEM for conventional imaging, together with studying the β -phase by XRD, FTIR, or Raman spectroscopy. These last three methods can be combined or may complement each other. For electrical properties investigations, the piezoelectric coefficient d_{33} , which appears in almost every electrical characterization, and the permittivity of the material are measured.

In spite of that, many papers do not discuss a reasonably important topic, and that is degradation. Therefore, it raises many questions for newly created materials. How long will these materials retain their stability? How much stress can they withstand, and what else is harmful to them? This is especially relevant in combination with perovskites. Since their primary use is as PENG, TENG, or combinations of these, increasing the mechanical stress is to be expected. Even though PVDF is in some aspects a durable polymer, it should not be relied upon entirely on this fact, given that its use is highly specific to each experiment. It is thus appropriate to use accelerated aging degradation tests to verify that the design can be utilized more than just on an experimental level.

Hence, in future years, there is expected to be a continuing trend of almost exponential growth in the development of this material, expanding the scope and commercialization of such nanogenerators for specific applications.

Author Contributions: Conceptualization, N.P., R.D. and D.S.; software, N.P.; validation, T.P. and E.Š.; formal analysis, Š.Ť. and K.Č.; resources, P.S. and K.Č.; writing—original draft preparation, N.P.; writing—review and editing, T.P., R.D. and N.P.; visualization, N.P.; project administration, Š.Ť.; funding acquisition, Š.Ť. and P.S. All authors have read and agreed to the published version of the manuscript.

Funding: Research described in the paper was financially supported by the Ministry of Education, Youth and Sports of the Czech Republic under the project CEITEC 2020 (LQ1601), by the Internal Grant Agency of Brno University of Technology, grant No. FEKT-S-20-6352, and by the Grant Agency of Czech Republic under project No. 19-17457S. Part of the work was carried out with the support of CEITEC Nano Research Infrastructure supported by MEYS CR (LM2018110).

Institutional Review Board Statement: Not applicable.

Informed Consent Statement: Not applicable.

Conflicts of Interest: The authors declare no conflicts of interest

Sample Availability: Data will be provided upon personal request to Nikola Papež. E-mail: papez@vut.cz.

Abbreviations

The following abbreviations are used in this manuscript:

AC	acetone
AFM	atomic force microscopy
ASTM	American Society for Testing and Materials
ATEC	acetyl triethyl citrate
ATR	attenuated total reflection
BET	Brunauer–Emmett–Teller
BN	boron nitride
CFE	chlorofluoroethylene
CHO	cyclohexanone
CPO	cyclopentanone
DBP	dibutyl phthalate
DBS	dibutyl sebacate
DEC	diethyl carbonate
DEP	diethyl phthalate
DMAc	dimethylacetamide
DMF	dimethyl formamide
DMSO	dimethylsulphoxide
DSC	differential scanning calorimetry
EDS	energy dispersive spectroscopy
FIB	focused ion beam
FEP	fluorinated ethylene propylene
FTIR	Fourier transform infrared spectroscopy
GBL	γ -butyrolactone
HMPA	hexamethyl phosphoramidate
IoT	internet of things
MEK	methyl ethyl ketone
NMP	<i>N</i> -methyl-2-pyrrolidone
PA6	nylon-6
PAN	polyacrylonitrile
PC	propylene carbonate
PFM	piezoresponse force microscopy
PZT	lead zirconate titanate
P&F	Press & Folding
UHD	ultrahigh definition
PENG	piezoelectric nanogenerator
PFM	piezoresponse force microscopy
PTFE	polytetrafluoroethylene
PMMA	poly(methyl methacrylate)
PVDF	polyvinylidene fluoride
PZT	lead zirconate titanate
SEM	scanning electron microscope
TBSA	<i>N,N'</i> -tetrabutylsuccindiamide
TEC	triethyl citrate
TEG	thermoelectric generator
TENG	triboelectric nanogenerator
TEP	triethyl phosphate
TGA	thermogravimetric analysis
THF	tetrahydrofuran
TMP	trimethyl phosphate
TMU	tetramethylurea
TrFE	trifluoroethylene
XPS	X-ray photoelectron spectroscopy
XRD	X-ray crystallography

References

1. Centa, U.G.; Mihelčič, M.; Bobnar, V.; Remškar, M.; Perše, L.S. The Effect of PVP on Thermal, Mechanical, and Dielectric Properties in PVDF-HFP/PVP Thin Film. *Coatings* **2022**, *12*, 1241. [[CrossRef](#)]
2. Zhang, S.; Shen, J.; Qiu, X.; Weng, D.; Zhu, W. ESR and vibrational spectroscopy study on poly(vinylidene fluoride) membranes with alkaline treatment. *J. Power Sources* **2006**, *153*, 234–238. [[CrossRef](#)]
3. Ren, Z.; Wang, Z.; Liu, Z.; Wang, L.; Guo, H.; Li, L.; Li, S.; Chen, X.; Tang, W.; Wang, Z.L. Energy Harvesting from Breeze Wind (0.7–6 m s⁻¹) Using Ultra-Stretchable Triboelectric Nanogenerator. *Adv. Energy Mater.* **2020**, *10*, 2001770. [[CrossRef](#)]
4. Ren, Z.; Ding, Y.; Nie, J.; Wang, F.; Xu, L.; Lin, S.; Chen, X.; Wang, Z.L. Environmental Energy Harvesting Adapting to Different Weather Conditions and Self-Powered Vapor Sensor Based on Humidity-Responsive Triboelectric Nanogenerators. *ACS Appl. Mater. Interfaces* **2019**, *11*, 6143–6153. [[CrossRef](#)]
5. Ren, Z.; Wang, Z.; Wang, F.; Li, S.; Wang, Z.L. Vibration behavior and excitation mechanism of ultra-stretchable triboelectric nanogenerator for wind energy harvesting. *Extrem. Mech. Lett.* **2021**, *45*, 101285. [[CrossRef](#)]
6. Tofel, P.; Částková, K.; Říha, D.; Sobola, D.; Papež, N.; Kaštyl, J.; Ťálu, Š.; Hadaš, Z. Triboelectric Response of Electrospun Stratified PVDF and PA Structures. *Nanomaterials* **2022**, *12*, 349. [[CrossRef](#)]
7. Singh, H.H.; Khare, N. Flexible ZnO-PVDF/PTFE based piezo-tribo hybrid nanogenerator. *Nano Energy* **2018**, *51*, 216–222. [[CrossRef](#)]
8. Mariello, M. Recent Advances on Hybrid Piezo-Triboelectric Bio-Nanogenerators: Materials, Architectures and Circuitry. *Nanoenergy Adv.* **2022**, *2*, 4. [[CrossRef](#)]
9. Wang, X.; Yang, B.; Liu, J.; Zhu, Y.; Yang, C.; He, Q. A flexible triboelectric-piezoelectric hybrid nanogenerator based on P(VDF-TrFE) nanofibers and PDMS/MWCNT for wearable devices. *Sci. Rep.* **2016**, *6*, 36409. [[CrossRef](#)]
10. Jung, W.S.; Kang, M.G.; Moon, H.G.; Baek, S.H.; Yoon, S.J.; Wang, Z.L.; Kim, S.W.; Kang, C.Y. High Output Piezo/Triboelectric Hybrid Generator. *Sci. Rep.* **2015**, *5*, 9309. [[CrossRef](#)]
11. Lapčinskis, L.; Mā Lnieks, K.; Linarts, A.; Blū Ms, J.; Šmits, K.N.; Järvekūlg, M.; Knite, M.R.; Šutka, A. Hybrid Tribo-Piezo-Electric Nanogenerator with Unprecedented Performance Based on Ferroelectric Composite Contacting Layers. *ACS Appl. Energy Mater.* **2019**, *2*, 4027–4032. [[CrossRef](#)]
12. Ren, Z.; Nie, J.; Shao, J.; Lai, Q.; Wang, L.; Chen, J.; Chen, X.; Lin Wang, Z.; Ren, Z.; Nie, J.; et al. Fully Elastic and Metal-Free Tactile Sensors for Detecting both Normal and Tangential Forces Based on Triboelectric Nanogenerators. *Adv. Funct. Mater.* **2018**, *28*, 1802989. [[CrossRef](#)]
13. Bohlén, M.; Bolton, K. Conformational studies of poly(vinylidene fluoride), poly(trifluoroethylene) and poly(vinylidene fluoride-co-trifluoroethylene) using density functional theory. *Phys. Chem. Chem. Phys.* **2014**, *16*, 12929–12939. [[CrossRef](#)] [[PubMed](#)]
14. Ruan, L.; Yao, X.; Chang, Y.; Zhou, L.; Qin, G.; Zhang, X. Properties and Applications of the β Phase Poly(vinylidene fluoride). *Polymers* **2018**, *10*, 228. [[CrossRef](#)]
15. McKeen, L. *Film Properties of Plastics and Elastomers*, 3rd ed.; William Andrew Publishing: Boston, MA, USA, 2012; p. 408. [[CrossRef](#)]
16. Song, R.; Yang, D.; He, L. Effect of surface modification of nanosilica on crystallization, thermal and mechanical properties of poly(vinylidene fluoride). *J. Mater. Sci.* **2007**, *42*, 8408–8417. [[CrossRef](#)]
17. Pisarenko, T.; Papež, N.; Sobola, D.; Ťálu, Š.; Částková, K.; Škarvada, P.; Macků, R.; Ščasnovič, E.; Kaštyl, J. Comprehensive Characterization of PVDF Nanofibers at Macro- and Nanolevel. *Polymers* **2022**, *14*, 593. [[CrossRef](#)]
18. Lin, Y.; Zhang, Y.; Zhang, F.; Zhang, M.; Li, D.; Deng, G.; Guan, L.; Dong, M. Studies on the electrostatic effects of stretched PVDF films and nanofibers. *Nanoscale Res. Lett.* **2021**, *16*, 79. [[CrossRef](#)]
19. Saxena, P.; Shukla, P. A comprehensive review on fundamental properties and applications of poly(vinylidene fluoride) (PVDF). *Adv. Compos. Hybrid Mater.* **2021**, *4*, 8–26. [[CrossRef](#)]
20. Kang, G.-d.; ming Cao, Y. Application and modification of poly(vinylidene fluoride) (PVDF) membranes—A review. *J. Membr. Sci.* **2014**, *463*, 145–165. [[CrossRef](#)]
21. Xin, Y.; Zhu, J.; Sun, H.; Xu, Y.; Liu, T.; Qian, C. A brief review on piezoelectric PVDF nanofibers prepared by electrospinning. *Ferroelectrics* **2018**, *526*, 140–151. [[CrossRef](#)]
22. Atif, R.; Khaliq, J.; Combrinck, M.; Hassanin, A.H.; Shehata, N.; Elnabawy, E.; Shyha, I. Solution Blow Spinning of Polyvinylidene Fluoride Based Fibers for Energy Harvesting Applications: A Review. *Polymers* **2020**, *12*, 1304. [[CrossRef](#)] [[PubMed](#)]
23. Wang, Y.; Zhu, L.; Du, C. Progress in Piezoelectric Nanogenerators Based on PVDF Composite Films. *Micromachines* **2021**, *12*, 1278. [[CrossRef](#)] [[PubMed](#)]
24. He, Z.; Rault, F.; Lewandowski, M.; Mohsenzadeh, E.; Salaün, F. Electrospun PVDF nanofibers for piezoelectric applications: A review of the influence of electrospinning parameters on the β phase and crystallinity enhancement. *Polymers* **2021**, *13*, 174. [[CrossRef](#)]
25. Liu, F.; Hashim, N.A.; Liu, Y.; Abed, M.R.; Li, K. Progress in the production and modification of PVDF membranes. *J. Membr. Sci.* **2011**, *375*, 1–27. [[CrossRef](#)]
26. Wu, L.; Jin, Z.; Liu, Y.; Ning, H.; Liu, X.; Alamusi.; Hu, N. Recent advances in the preparation of PVDF-based piezoelectric materials. *Nanotechnol. Rev.* **2022**, *11*, 1386–1407. [[CrossRef](#)]
27. Palazzetti, R.; Zucchelli, A. Electrospun nanofibers as reinforcement for composite laminates materials—A review. *Compos. Struct.* **2017**, *182*, 711–727. [[CrossRef](#)]

28. Fotouhi, M.; Saghafi, H.; Brugo, T.; Minak, G.; Fragassa, C.; Zucchelli, A.; Ahmadi, M. Effect of PVDF nanofibers on the fracture behavior of composite laminates for high-speed woodworking machines. *Proc. Inst. Mech. Eng. Part J. Mech. Eng. Sci.* **2016**, *231*, 31–43. [[CrossRef](#)]
29. Wu, Q.; Tiraferri, A.; Wu, H.; Xie, W.; Liu, B. Improving the Performance of PVDF/PVDF-g-PEGMA Ultrafiltration Membranes by Partial Solvent Substitution with Green Solvent Dimethyl Sulfoxide during Fabrication. *ACS Omega* **2019**, *4*, 19799–19807. [[CrossRef](#)]
30. Částková, K.; Kastyl, J.; Sobola, D.; Petruš, J.; Šťastná, E.; Říha, D.; Tofel, P. Structure–Properties Relationship of Electrospun PVDF Fibers. *Nanomaterials* **2020**, *10*, 1221. [[CrossRef](#)]
31. Gee, S.; Johnson, B.; Smith, A.L. Optimizing electrospinning parameters for piezoelectric PVDF nanofiber membranes. *J. Membr. Sci.* **2018**, *563*, 804–812. [[CrossRef](#)]
32. Ghafari, E.; Jiang, X.; Lu, N. Surface morphology and β -phase formation of single polyvinylidene fluoride (PVDF) composite nanofibers. *Adv. Compos. Hybrid Mater.* **2017**, *1*, 332–340. [[CrossRef](#)]
33. Shao, H.; Fang, J.; Wang, H.; Lin, T. Effect of electrospinning parameters and polymer concentrations on mechanical-to-electrical energy conversion of randomly-oriented electrospun poly(vinylidene fluoride) nanofiber mats. *RSC Adv.* **2015**, *5*, 14345–14350. [[CrossRef](#)]
34. Fu, R.; Chen, S.; Lin, Y.; He, Y.; Gu, Y. Preparation and piezoelectric investigation of electrospun polyvinylidene fluoride fibrous membrane. *J. Nanosci. Nanotechnol.* **2016**, *16*, 12337–12343. [[CrossRef](#)]
35. Magniez, K.; De Lavigne, C.; Fox, B.L. The effects of molecular weight and polymorphism on the fracture and thermo-mechanical properties of a carbon-fibre composite modified by electrospun poly(vinylidene fluoride) membranes. *Polymer* **2010**, *12*, 2585–2596. [[CrossRef](#)]
36. Zaarour, B.; Zhu, L.; Jin, X. Controlling the surface structure, mechanical properties, crystallinity, and piezoelectric properties of electrospun PVDF nanofibers by maneuvering molecular weight. *Soft Mater.* **2019**, *17*, 181–189. [[CrossRef](#)]
37. Lei, T.; Yu, L.; Zheng, G.; Wang, L.; Wu, D.; Sun, D. Electrospinning-induced preferred dipole orientation in PVDF fibers. *J. Mater. Sci.* **2015**, *50*, 4342–4347. [[CrossRef](#)]
38. Liu, Z.H.; Pan, C.T.; Lin, L.W.; Huang, J.C.; Ou, Z.Y. Direct-write PVDF nonwoven fiber fabric energy harvesters via the hollow cylindrical near-field electrospinning process. *Smart Mater. Struct.* **2013**, *23*, 025003. [[CrossRef](#)]
39. Wang, Y.R.; Zheng, J.M.; Ren, G.Y.; Zhang, P.H.; Xu, C. A flexible piezoelectric force sensor based on PVDF fabrics. *Smart Mater. Struct.* **2011**, *20*, 045009. [[CrossRef](#)]
40. Mokhtari, F.; Shamsirsaz, M.; Latifi, M.; Foroughi, J. Nanofibers-Based Piezoelectric Energy Harvester for Self-Powered Wearable Technologies. *Polymers* **2020**, *12*, 2697. [[CrossRef](#)]
41. Hansen, C.M. *Hansen Solubility Parameters: A User's Handbook*, 2nd ed.; CRC Press: Boca Raton, FL, USA, 2007; p. 544. [[CrossRef](#)]
42. Egemen, E.; Nirmalakhandan, N.; Trevizo, C. Predicting surface tension of liquid organic solvents. *Environ. Sci. Technol.* **2000**, *34*, 2596–2600. [[CrossRef](#)]
43. Marshall, J.E.; Zhenova, A.; Roberts, S.; Petchey, T.; Zhu, P.; Dancer, C.E.; McElroy, C.R.; Kendrick, E.; Goodship, V. On the Solubility and Stability of Polyvinylidene Fluoride. *Polymers* **2021**, *13*, 1354. [[CrossRef](#)] [[PubMed](#)]
44. Zhou, Y.; Zhang, S.; Xu, X.; Liu, W.; Zhang, S.; Li, G.; He, J. Dynamic piezo-thermoelectric generator for simultaneously harvesting mechanical and thermal energies. *Nano Energy* **2020**, *69*, 104397. [[CrossRef](#)]
45. Li, Y.; Liao, C.; Tjong, S.C. Electrospun Polyvinylidene Fluoride-Based Fibrous Scaffolds with Piezoelectric Characteristics for Bone and Neural Tissue Engineering. *Nanomaterials* **2019**, *9*, 952. [[CrossRef](#)] [[PubMed](#)]
46. Li, B.M.; Ju, B.; Zhou, Y.; Knowles, C.G.; Rosenberg, Z.; Flewellin, T.J.; Kose, F.; Jur, J.S. Airbrushed PVDF-TrFE Fibrous Sensors for E-Textiles. *ACS Appl. Electron. Mater.* **2021**, *3*, 5307–5326. [[CrossRef](#)]
47. Cho, E.; Kim, C.; Kook, J.K.; Jeong, Y.I.; Kim, J.H.; Kim, Y.A.; Endo, M.; Hwang, C.H. Fabrication of electrospun PVDF nanofiber membrane for Western blot with high sensitivity. *J. Membr. Sci.* **2012**, *389*, 349–354. [[CrossRef](#)]
48. Gupta, V.; Babu, A.; Ghosh, S.K.; Mallick, Z.; Mishra, H.K.; Saini, D.; Mandal, D. Revisiting δ -PVDF based piezoelectric nanogenerator for self-powered pressure mapping sensor. *Appl. Phys. Lett.* **2021**, *119*, 252902. [[CrossRef](#)]
49. Yu, L.; Zhou, P.; Wu, D.; Wang, L.; Lin, L.; Sun, D. Shoepad nanogenerator based on electrospun PVDF nanofibers. *Microsyst. Technol.* **2018**, *25*, 3151–3156. [[CrossRef](#)]
50. Sedlak, P.; Gajdos, A.; Macku, R.; Majzner, J.; Holcman, V.; Sedlakova, V.; Kubersky, P. The effect of thermal treatment on ac/dc conductivity and current fluctuations of PVDF/NMP/[EMIM][TFSI] solid polymer electrolyte. *Sci. Rep.* **2020**, *10*, 21140. [[CrossRef](#)]
51. Kalimuldina, G.; Turdakyn, N.; Abay, I.; Medeubayev, A.; Nurpeissova, A.; Adair, D.; Bakenov, Z. A Review of Piezoelectric PVDF Film by Electrospinning and Its Applications. *Sensors* **2020**, *20*, 5214. [[CrossRef](#)]
52. Sengupta, A.; Das, S.; Dasgupta, S.; Sengupta, P.; Datta, P. Flexible Nanogenerator from Electrospun PVDF-Polycarbazole Nanofiber Membranes for Human Motion Energy-Harvesting Device Applications. *ACS Biomater. Sci. Eng.* **2021**, *7*, 1673–1685. doi: 10.1021/acsbomaterials.0c01730. [[CrossRef](#)]
53. Shi, L.; Jin, H.; Dong, S.; Huang, S.; Kuang, H.; Xu, H.; Chen, J.; Xuan, W.; Zhang, S.; Li, S.; et al. High-performance triboelectric nanogenerator based on electrospun PVDF-graphene nanosheet composite nanofibers for energy harvesting. *Nano Energy* **2021**, *80*, 105599. [[CrossRef](#)]
54. Li, C.; Wang, H.; Yan, X.; Chen, H.; Fu, Y.; Meng, Q. Enhancement Research on Piezoelectric Performance of Electrospun PVDF Fiber Membranes with Inorganic Reinforced Materials. *Coatings* **2021**, *11*, 1495. [[CrossRef](#)]

55. Costa, L.M.M.; Bretas, R.E.S.; Gregorio, R.; Costa, L.M.M.; Bretas, R.E.S.; Gregorio, R. Effect of Solution Concentration on the Electrospay/Electrospinning Transition and on the Crystalline Phase of PVDF. *Mater. Sci. Appl.* **2010**, *1*, 247–252. [[CrossRef](#)]
56. Correia, D.M.; Gonçalves, R.; Ribeiro, C.; Sencadas, V.; Botelho, G.; Ribelles, J.L.; Lanceros-Méndez, S. Electrospayed poly(vinylidene fluoride) microparticles for tissue engineering applications. *RSC Adv.* **2014**, *4*, 33013–33021. [[CrossRef](#)]
57. Kliem, H.; Tadros-Morgane, R. Extrinsic versus intrinsic ferroelectric switching: Experimental investigations using ultra-thin PVDF Langmuir–Blodgett films. *J. Phys. Appl. Phys.* **2005**, *38*, 1860. [[CrossRef](#)]
58. Chen, S.; Li, X.; Yao, K.; Tay, F.E.H.; Kumar, A.; Zeng, K. Self-polarized ferroelectric PVDF homopolymer ultra-thin films derived from Langmuir–Blodgett deposition. *Polymer* **2012**, *53*, 1404–1408. [[CrossRef](#)]
59. Cozza, E.S.; Monticelli, O.; Marsano, E.; Cebe, P. On the electrospinning of PVDF: Influence of the experimental conditions on the nanofiber properties. *Polym. Int.* **2013**, *62*, 41–48. [[CrossRef](#)]
60. Motamedi, A.S.; Mirzadeh, H.; Hajiesmaeilbaigi, F.; Bagheri-Khoulenjani, S.; Shokrgozar, M.A. Effect of electrospinning parameters on morphological properties of PVDF nanofibrous scaffolds. *Prog. Biomater.* **2017**, *6*, 113–123. [[CrossRef](#)]
61. Černohorský, P.; Pisarenko, T.; Papež, N.; Sobola, D.; Ťálu, Š.; Částková, K.; Kaštyl, J.; Macků, R.; Škarvada, P.; Sedlák, P. Structure Tuning and Electrical Properties of Mixed PVDF and Nylon Nanofibers. *Materials* **2021**, *14*, 6096. [[CrossRef](#)]
62. Yu, Z.; Chen, M.; Wang, Y.; Zheng, J.; Zhang, Y.; Zhou, H.; Li, D. Nanoporous PVDF Hollow Fiber Employed Piezo-Tribo Nanogenerator for Effective Acoustic Harvesting. *ACS Appl. Mater. Interfaces* **2021**, *13*, 26981–26988. [[CrossRef](#)]
63. Na, H.; Chen, P.; Wong, S.C.; Hague, S.; Li, Q. Fabrication of PVDF/PVA microtubules by coaxial electrospinning. *Polymer* **2012**, *53*, 2736–2743. [[CrossRef](#)]
64. Ponnamma, D.; Chamakh, M.M.; Alahzm, A.M.; Salim, N.; Hameed, N.; Almaadeed, M.A.A. Core-Shell Nanofibers of Polyvinylidene Fluoride-based Nanocomposites as Piezoelectric Nanogenerators. *Polymers* **2020**, *12*, 2344. [[CrossRef](#)]
65. Asai, H.; Kikuchi, M.; Shimada, N.; Nakane, K. Effect of melt and solution electrospinning on the formation and structure of poly(vinylidene fluoride) fibres. *RSC Adv.* **2017**, *7*, 17593–17598. [[CrossRef](#)]
66. Fontananova, E.; Bahattab, M.A.; Aljlil, S.A.; Alowairdy, M.; Rinaldi, G.; Vuono, D.; Nagy, J.B.; Drioli, E.; Di Profio, G. From hydrophobic to hydrophilic polyvinylidene fluoride (PVDF) membranes by gaining new insight into material's properties. *RSC Adv.* **2015**, *5*, 56219–56231. [[CrossRef](#)]
67. Hamad, M.E.; Al-Gharabli, S.; Kujawa, J. Tunable hydrophobicity and roughness on PVDF surface by grafting to mode—Approach to enhance membrane performance in membrane distillation process. *Sep. Purif. Technol.* **2022**, *291*, 120935. [[CrossRef](#)]
68. Sheikh, F.A.; Cantu, T.; Macossay, J.; Kim, H. Fabrication of Poly(vinylidene fluoride) (PVDF) Nanofibers Containing Nickel Nanoparticles as Future Energy Server Materials. *Sci. Adv. Mater.* **2011**, *3*, 216–222. [[CrossRef](#)]
69. Issa, A.; Al-Maadeed, M.; Luyt, A.; Ponnamma, D.; Hassan, M. Physico-Mechanical, Dielectric, and Piezoelectric Properties of PVDF Electrospun Mats Containing Silver Nanoparticles. *C J. Carbon Res.* **2017**, *3*, 30. [[CrossRef](#)]
70. Mokhtari, F.; Spinks, G.M.; Fay, C.; Cheng, Z.; Raad, R.; Xi, J.; Foroughi, J. Wearable Electronic Textiles from Nanostructured Piezoelectric Fibers. *Adv. Mater. Technol.* **2020**, *5*, 1900900. [[CrossRef](#)]
71. Ji, J.; Liu, F.; Hashim, N.A.; Abed, M.R.; Li, K. Poly(vinylidene fluoride) (PVDF) membranes for fluid separation. *React. Funct. Polym.* **2015**, *86*, 134–153. [[CrossRef](#)]
72. Shen, L.; Feng, S.; Li, J.; Chen, J.; Li, F.; Lin, H.; Yu, G. Surface modification of polyvinylidene fluoride (PVDF) membrane via radiation grafting: novel mechanisms underlying the interesting enhanced membrane performance. *Sci. Rep.* **2017**, *7*, 2721. [[CrossRef](#)]
73. He, Z.; Rault, F.; Vishwakarma, A.; Mohsenzadeh, E.; Salaün, F. High-Aligned PVDF Nanofibers with a High Electroactive Phase Prepared by Systematically Optimizing the Solution Property and Process Parameters of Electrospinning. *Coatings* **2022**, *12*, 1310. [[CrossRef](#)]
74. Sobola, D.; Kaspar, P.; Částková, K.; Dallaev, R.; Papež, N.; Sedlák, P.; Trčka, T.; Orudzhev, F.; Kaštyl, J.; Weiser, A.; et al. PVDF Fibers Modification by Nitrate Salts Doping. *Polymers* **2021**, *13*, 2439. [[CrossRef](#)] [[PubMed](#)]
75. Tubio, C.R.; Costa, P.; Nguyen, D.N.; Moon, W. Significant Electromechanical Characteristic Enhancement of Coaxial Electrospinning Core-Shell Fibers. *Polymers* **2022**, *14*, 1739. [[CrossRef](#)]
76. Sharma, T.; Naik, S.; Langevine, J.; Gill, B.; Zhang, J.X. Aligned PVDF-TrFE nanofibers with high-density PVDF nanofibers and PVDF core-shell structures for endovascular pressure sensing. *IEEE Trans. Biomed. Eng.* **2015**, *62*, 188–195. [[CrossRef](#)]
77. Wang, S.; Shi, K.; Chai, B.; Qiao, S.; Huang, Z.; Jiang, P.; Huang, X. Core-shell structured silk Fibroin/PVDF piezoelectric nanofibers for energy harvesting and self-powered sensing. *Nano Mater. Sci.* **2022**, *4*, 126–132. [[CrossRef](#)]
78. Horchidan, N.; Ciomaga, C.E.; Curecheriu, L.P.; Stoian, G.; Botea, M.; Florea, M.; Maraloiu, V.A.; Pintilie, L.; Tufescu, F.M.; Tiron, V.; et al. Increasing Permittivity and Mechanical Harvesting Response of PVDF-Based Flexible Composites by Using Ag Nanoparticles onto BaTiO₃ Nanofillers. *Nanomaterials* **2022**, *12*, 934. [[CrossRef](#)]
79. Mendes, S.F.; Costa, C.M.; Caparros, C.; Sencadas, V.; Lanceros-Méndez, S. Effect of filler size and concentration on the structure and properties of poly(vinylidene fluoride)/BaTiO₃ nanocomposites. *J. Mater. Sci.* **2012**, *47*, 1378–1388. [[CrossRef](#)]
80. Lee, Y.J.; Jeong, S.K.; Jo, N.J. PVDF-Based Nanocomposite Solid Polymer Electrolytes; the Effect of Affinity Between PVDF and Filler on Ionic Conductivity. *Compos. Interfaces* **2012**, *16*, 347–358. [[CrossRef](#)]
81. Li, Y.; Wang, Z.; Li, Y.; Yi, Z. Enhanced breakdown strength of PVDF textile composites by BiFeO₃ fibers in low loading. *J. Mater. Sci. Mater. Electron.* **2022**, *33*, 3215–3224. [[CrossRef](#)]
82. Ichangi, A.; Khan, L.; Queraltó, A.; Grosch, M.; Weißing, R.; Ünlü, F.; Chijioke, A.K.; Verma, A.; Fischer, T.; Surmenev, R.; et al. Electrospun BiFeO₃ Nanofibers for Vibrational Energy Harvesting Application. *Adv. Eng. Mater.* **2021**, *24*, 2101394. [[CrossRef](#)]

83. Hu, X.; Che, Y.; Zhang, Z.; Shen, Q.D.; Chu, B. BiFeO₃-BaTiO₃/P(VDF-TrFE) Multifunctional Polymer Nanocomposites. *ACS Appl. Electron. Mater.* **2021**, *3*, 743–751. [[CrossRef](#)]
84. Ramazanov, S.; Sobola, D.; Orudzhev, F.; Knápek, A.; Polčák, J.; Potoček, M.; Kaspar, P.; Dallaev, R. Surface Modification and Enhancement of Ferromagnetism in BiFeO₃ Nanofilms Deposited on HOPG. *Nanomaterials* **2020**, *10*, 1990. [[CrossRef](#)] [[PubMed](#)]
85. Kalani, S.; Kohandani, R.; Bagherzadeh, R. Flexible electrospun PVDF–BaTiO₃ hybrid structure pressure sensor with enhanced efficiency. *RSC Adv.* **2020**, *10*, 35090–35098. [[CrossRef](#)]
86. Kumar, M.; Kulkarni, N.D.; Kumari, P. Fabrication and characterization of PVDF/BaTiO₃ nanocomposite for energy harvesting application. *Mater. Today Proc.* **2022**, *56*, 1151–1155. [[CrossRef](#)]
87. Abdolmaleki, H.; Agarwala, S. PVDF–BaTiO₃ Nanocomposite Inkjet Inks with Enhanced β -Phase Crystallinity for Printed Electronics. *Polymers* **2020**, *12*, 2430. [[CrossRef](#)]
88. Ramesh, D.; D'Souza, N.A. One-step fabrication of biomimetic PVDF–BaTiO₃ nanofibrous composite using DoE. *Mater. Res. Express* **2018**, *5*, 085308. [[CrossRef](#)]
89. Sreejivungsa, K.; Phromviyo, N.; Swatsitang, E.; Thongbai, P. Characterizations and Significantly Enhanced Dielectric Properties of PVDF Polymer Nanocomposites by Incorporating Gold Nanoparticles Deposited on BaTiO₃ Nanoparticles. *Polymers* **2021**, *13*, 4144. [[CrossRef](#)]
90. Wang, J.; Hu, J.; Sun, Q.; Zhu, K.; Li, B.W.; Qiu, J. Dielectric and energy storage performances of PVDF-based composites with colossal permittivity Nd-doped BaTiO₃ nanoparticles as the filler. *AIP Adv.* **2017**, *7*, 125104. [[CrossRef](#)]
91. Hussein, A.D.; Sabry, R.S.; Abdul Azeed Dakhil, O.; Bagherzadeh, R. Effect of Adding BaTiO₃ to PVDF as Nano Generator. *J. Phys. Conf. Ser.* **2019**, *1294*, 022012. [[CrossRef](#)]
92. Ma, J.; Zhang, Q.; Lin, K.; Zhou, L.; Ni, Z. Piezoelectric and optoelectronic properties of electrospinning hybrid PVDF and ZnO nanofibers. *Mater. Res. Express* **2018**, *5*, 35057. [[CrossRef](#)]
93. Li, G.Y.; Zhang, H.D.; Guo, K.; Ma, X.S.; Long, Y.Z. Fabrication and piezoelectric-pyroelectric properties of electrospun PVDF/ZnO composite fibers. *Mater. Res. Express* **2020**, *7*, 095502. [[CrossRef](#)]
94. Yun, J.S.; Park, C.K.; Jeong, Y.H.; Cho, J.H.; Paik, J.H.; Yoon, S.H.; Hwang, K.R. The Fabrication and Characterization of Piezoelectric PZT/PVDF Electrospun Nanofiber Composites. *Nanomater. Nanotechnol.* **2016**, *6*, 20. [[CrossRef](#)]
95. He, W.; Guo, Y.; Zhao, Y.B.; Jiang, F.; Schmitt, J.; Yue, Y.; Liu, J.; Cao, J.; Wang, J. Self-supporting smart air filters based on PZT/PVDF electrospun nanofiber composite membrane. *Chem. Eng. J.* **2021**, *423*, 130247. [[CrossRef](#)]
96. Fortunato, M.; Cavallini, D.; De Bellis, G.; Marra, F.; Tamburrano, A.; Sarto, F.; Sarto, M.S. Phase Inversion in PVDF Films with Enhanced Piezoresponse Through Spin-Coating and Quenching. *Polymers* **2019**, *11*, 1096. [[CrossRef](#)] [[PubMed](#)]
97. Salimi, A.; Yousefi, A.A. Analysis Method: FTIR studies of β -phase crystal formation in stretched PVDF films. *Polym. Test.* **2003**, *22*, 699–704. [[CrossRef](#)]
98. Lim, J.Y.; Kim, S.; Seo, Y. Enhancement of β -phase in PVDF by electrospinning. *AIP Conf. Proc.* **2015**, *1664*, 070006. [[CrossRef](#)]
99. Kabir, E.; Khatun, M.; Nasrin, L.; Raihan, M.J.; Rahman, M. Pure β -phase formation in polyvinylidene fluoride (PVDF)-carbon nanotube composites. *J. Phys. Appl. Phys.* **2017**, *50*, 163002. [[CrossRef](#)]
100. Vasic, N.; Steinmetz, J.; Görke, M.; Sinapius, M.; Hühne, C.; Garnweitner, G. Phase Transitions of Polarised PVDF Films in a Standard Curing Process for Composites. *Polymers* **2021**, *13*, 3900. [[CrossRef](#)]
101. Meng, N.; Ren, X.; Santagiuliana, G.; Ventura, L.; Zhang, H.; Wu, J.; Yan, H.; Reece, M.J.; Bilotti, E. Ultrahigh β -phase content poly(vinylidene fluoride) with relaxor-like ferroelectricity for high energy density capacitors. *Nat. Commun.* **2019**, *10*, 4535. [[CrossRef](#)]
102. Sedlak, P.; Sobola, D.; Gajdos, A.; Dallaev, R.; Nebojsa, A.; Kubersky, P. Surface Analyses of PVDF/NMP/[EMIM][TFSI] Solid Polymer Electrolyte. *Polymers* **2021**, *13*, 2678. [[CrossRef](#)]
103. Naga Kumar, C.; Prabhakar, M.N.; il Song, J. Synthesis of vinyl ester resin-carrying PVDF green nanofibers for self-healing applications. *Sci. Rep.* **2021**, *11*, 908. [[CrossRef](#)] [[PubMed](#)]
104. Victor, F.S.; Kugarajah, V.; Bangaru, M.; Ranjan, S.; Dharmalingam, S. Electrospun nanofibers of polyvinylidene fluoride incorporated with titanium nanotubes for purifying air with bacterial contamination. *Environ. Sci. Pollut. Res.* **2021**, *28*, 37520–37533. [[CrossRef](#)] [[PubMed](#)]
105. Sheikh, F.A.; Zargar, M.A.; Tamboli, A.H.; Kim, H. A super hydrophilic modification of poly(vinylidene fluoride) (PVDF) nanofibers: By in situ hydrothermal approach. *Appl. Surf. Sci.* **2016**, *385*, 417–425. [[CrossRef](#)]
106. Ding, R.; Wong, M.C.; Hao, J. Recent advances in hybrid perovskite nanogenerators. *EcoMat* **2020**, *2*, e12057. [[CrossRef](#)]
107. Abdullah, I.Y.; Yahaya, M.; Jumali, M.H.H.; Shanshool, H.M. Effect of annealing process on the phase formation in Poly(vinylidene fluoride) thin films. *AIP Conf. Proc.* **2014**, *1614*, 147–151. [[CrossRef](#)]
108. Mohd Dahan, R.; Arshad, A.N.; Mohamed, N.A.; Engku Zawawi, E.Z.; Kamarun, D.; Wahid, M.H.; Sarip, M.N.; Rusop Mahmood, M. ATR-FTIR Analysis on Polymorphism of PVDF/MgO Nanocomposite Thin Films. *Adv. Mater. Res.* **2016**, *1134*, 39–43. [[CrossRef](#)]
109. Nakhowong, R. Fabrication of PVDF/PVP nanofiltration membrane containing chitosan/activated carbon/Ag nanoparticles by electrospinning and their antibacterial activity. *SNRU J. Sci. Technol.* **2020**, *12*, 137–145.
110. Bai, H.; Wang, X.; Zhou, Y.; Zhang, L. Preparation and characterization of poly(vinylidene fluoride) composite membranes blended with nano-crystalline cellulose. *Prog. Nat. Sci. Mater. Int.* **2012**, *22*, 250–257. [[CrossRef](#)]
111. Lanceros-Méndez, S.; Mano, J.F.; Costa, A.M.; Schmidt, V.H. FTIR and DSC studies of mechanically deformed β -PVDF films. *J. Macromol. Sci. Part B* **2007**, *40 B*, 517–527. [[CrossRef](#)]

112. Chapron, D.; Rault, F.; Talbourdet, A.; Lemort, G.; Cochrane, C.; Bourson, P.; Devaux, E.; Campagne, C. In-situ Raman monitoring of the poly(vinylidene fluoride) crystalline structure during a melt-spinning process. *J. Raman Spectrosc.* **2021**, *52*, 1073–1079. [[CrossRef](#)]
113. Kobayashi, M.; Tashiro, K.; Tadokoro, H. Molecular Vibrations of Three Crystal Forms of Poly(vinylidene fluoride). *Macromolecules* **1975**, *8*, 158–171. [[CrossRef](#)]
114. Chipara, D.; Kuncser, V.; Lozano, K.; Alcoutlabi, M.; Ibrahim, E.; Chipara, M. Spectroscopic investigations on PVDF-Fe₂O₃ nanocomposites. *J. Appl. Polym. Sci.* **2020**, *137*, 48907. [[CrossRef](#)]
115. Shepelin, N.A.; Glushenkov, A.M.; Lussini, V.C.; Fox, P.J.; Dicinowski, G.W.; Shapter, J.G.; Ellis, A.V. New developments in composites, copolymer technologies and processing techniques for flexible fluoropolymer piezoelectric generators for efficient energy harvesting. *Energy Environ. Sci.* **2019**, *12*, 1143–1176. [[CrossRef](#)]
116. Tabari, R.S.; Chen, Y.; Thummavichai, K.; Zhang, Y.; Saadi, Z.; Neves, A.I.; Xia, Y.; Zhu, Y. Piezoelectric Property of Electrospun PVDF Nanofibers as Linking Tips of Artificial-Hair-Cell Structures in Cochlea. *Nanomaterials* **2022**, *12*, 1466. [[CrossRef](#)]
117. Moazeni, N.; Latifi, M.; Merati, A.A.; Rouhani, S. Crystal polymorphism in polydiacetylene-embedded electrospun polyvinylidene fluoride nanofibers. *Soft Matter* **2017**, *13*, 8178–8187. [[CrossRef](#)]
118. Saha, S.; Yauvana, V.; Chakraborty, S.; Sanyal, D. Synthesis and Characterization of Polyvinylidene-fluoride (PVDF) Nanofiber for Application as Piezoelectric Force Sensor. *Mater. Today Proc.* **2019**, *18*, 1450–1458. [[CrossRef](#)]
119. Chethan, P.B.; Renukappa, N.M.; Sanjeev, G. Preparation and crystalline studies of PVDF hybrid composites. *AIP Conf. Proc.* **2018**, *1942*, 050066. [[CrossRef](#)]
120. Huang, F.; Wei, Q.; Wang, J.; Cai, Y.; Huang, Y. Effect of temperature on structure, morphology and crystallinity of PVDF nanofibers via electrospinning. *e-Polymers* **2008**, *8*, 1–8. [[CrossRef](#)]
121. Liu, X.; Kuang, X.; Xu, S.; Wang, X. High-sensitivity piezoresponse force microscopy studies of single polyvinylidene fluoride nanofibers. *Mater. Lett.* **2017**, *191*, 189–192. [[CrossRef](#)]
122. Pisarenko, T. Characterization of PVDF nanofibers created by the electrospinning method. In Proceedings of the 26th Conference STUDENT EEICT 2020, Brno, Czech Republic, 23 April 2020; Vítězslav, N., Ed.; Brno University of Technology, Faculty of Electrical Engineering and Communication: Brno, Czech Republic, 2020; pp. 287–291.
123. Țălu, Ș. *Micro and Nanoscale Characterization of Three Dimensional Surfaces: Basics and Applications*; Napoca Star Publishing House: Cluj-Napoca, Romania, 2015.
124. Szewczyk, P.K.; Gradys, A.; Kim, S.K.; Persano, L.; Marzec, M.; Krysztal, A.; Busolo, T.; Toncelli, A.; Pisignano, D.; Bernasik, A.; et al. Enhanced Piezoelectricity of Electrospun Polyvinylidene Fluoride Fibers for Energy Harvesting. *ACS Appl. Mater. Interfaces* **2020**, *12*, 13575–13583. [[CrossRef](#)] [[PubMed](#)]
125. Tohluebaji, N.; Putson, C.; Muensit, N.; Yuennan, J. Electrostrictive and structural properties of poly(Vinylidene fluoride-hexafluoropropylene) composite nanofibers filled with polyaniline (emeraldine base). *Polymers* **2021**, *13*, 3250. [[CrossRef](#)] [[PubMed](#)]
126. Ren, X.; Meng, N.; Zhang, H.; Wu, J.; Abrahams, I.; Yan, H.; Bilotti, E.; Reece, M.J. Giant energy storage density in PVDF with internal stress engineered polar nanostructures. *Nano Energy* **2020**, *72*, 104662. [[CrossRef](#)]
127. Wang, T.; Peng, R.C.; Peng, W.; Dong, G.; Zhou, C.; Yang, S.; Zhou, Z.; Liu, M.; Wang, T.; Peng, R.C.; et al. 2–2 Type PVDF-Based Composites Interlayered by Epitaxial (111)-Oriented BTO Films for High Energy Storage Density. *Adv. Funct. Mater.* **2022**, *32*, 2108496. [[CrossRef](#)]
128. Jing, L.; Li, W.; Gao, C.; Li, M.; Fei, W. Achieving High Energy Storage Performance in Polymer-Based Composites with Opposite Double Heterojunction Via Electric Field Tailoring. *SSRN Electron. J.* **2022**. [[CrossRef](#)]
129. Meng, G.; She, J.; Wang, C.; Wang, W.; Pan, C.; Cheng, Y. Sandwich-Structured h-BN/PVDF/h-BN Film With High Dielectric Strength and Energy Storage Density. *Front. Chem.* **2022**, *10*, 681. [[CrossRef](#)]
130. Cui, Y.; Ma, Y.; Zhang, Y.; Lin, X.; Zhang, S.; Si, T.; Zhang, C. Effect of multilayer structure on energy storage characteristics of PVDF ferroelectric polymer In Proceedings of the 2022 4th International Conference on Intelligent Control, Measurement and Signal Processing (ICMSP), Hangzhou, China, 8–10 July 2022; pp. 582–586. [[CrossRef](#)]
131. Chi, Q.; Ma, T.; Zhang, Y.; Cui, Y.; Zhang, C.; Lin, J.; Wang, X.; Lei, Q. Significantly enhanced energy storage density for poly(vinylidene fluoride) composites by induced PDA-coated 0.5Ba(Zr_{0.2}Ti_{0.8})O₃–0.5(Ba_{0.7}Ca_{0.3})TiO₃ nanofibers. *J. Mater. Chem. A* **2017**, *5*, 16757–16766. [[CrossRef](#)]
132. Ye, H.; Jiang, H.; Luo, Z.; Xu, L. Elastic interface in few-layer graphene/poly(vinylidene fluoride-trifluoroethylene-chloroethoxyethylene) nanocomposite with improved polarization. *J. Appl. Polym. Sci.* **2022**, *139*, 52030. [[CrossRef](#)]
133. Wang, Q.; Zhang, J.; Zhang, Z.; Hao, Y.; Bi, K. Enhanced dielectric properties and energy storage density of PVDF nanocomposites by co-loading of BaTiO₃ and CoFe₂O₄ nanoparticles. *Adv. Compos. Hybrid Mater.* **2020**, *3*, 58–65. [[CrossRef](#)]
134. Hambal, Y.; Shvartsman, V.V.; Michiels, I.; Zhang, Q.; Lupascu, D.C. High Energy Storage Density in Nanocomposites of P(VDF-TrFE-CFE) Terpolymer and BaZr_{0.2}Ti_{0.8}O₃ Nanoparticles. *Materials* **2022**, *15*, 3151. [[CrossRef](#)]
135. Kumar, A.; Roy, A. Structural and electromechanical characterization of lead magnesium niobate-lead titanate (PMN-0.3PT) piezoceramic for energy harvesting applications. *arXiv* **2022**, arXiv:2205.04313. <https://doi.org/10.48550/arxiv.2205.04313>.
136. Han, M.; Chan, Y.C.; Liu, W.; Zhang, S.; Zhang, H. Low frequency PVDF piezoelectric energy harvester with combined *d*₃₁ and *d*₃₃ operating modes. In Proceedings of the 8th Annual IEEE International Conference on Nano/Micro Engineered and Molecular Systems, IEEE NEMS 2013, Suzhou, China, 7–10 April 2013, pp. 440–443. [[CrossRef](#)]

137. Ahmad, K.A.; Rahman, M.F.; Hussain, Z.; Osman, M.K.; Sulaiman, S.N.; Abdullah, M.F.; Abdullah, N.; Manaf, A.A. Design and development of D33 mode piezoelectric acoustic transducer array using PVDF for underwater application. In Proceedings of the 7th IEEE International Conference on Control System, Computing and Engineering, ICCSCE 2017, Penang, Malaysia, 24–26 November 2017; pp. 1–5. [[CrossRef](#)]
138. Zhou, W.; Lin, Y.; Zou, K.; Zhou, C.; Gong, X.; Cao, Y.; Jiang, S. Enhancement of piezoelectricity in polymer PVDF based on molecular chain structure. *J. Mater. Sci. Mater. Electron.* **2021**, *32*, 28708–28717. [[CrossRef](#)]
139. Zhang, C.; Wei, W.; Sun, H.; Zhu, Q. Performance enhancements in poly(vinylidene fluoride)-based piezoelectric films prepared by the extrusion-casting process. *J. Mater. Sci. Mater. Electron.* **2021**, *32*, 21837–21847. [[CrossRef](#)]
140. Chen, W.W.; An, Z.L.; He, L.B.; Deng, Z. Piezoelectric coefficients measurement for PVDF films with pneumatic pressure rig in a sole cavity. In Proceedings of the 2015 Symposium on Piezoelectricity, Acoustic Waves and Device Applications, SPAWDA 2015, Jinan, China, 30 October–2 November 2015; pp. 111–114. [[CrossRef](#)]
141. Li, J.F. *Lead-Free Piezoelectric Materials*; Wiley: Hoboken, NJ, USA, 2021; p. 242.
142. Bai, Z.; Song, Y.; Peng, J.; Chen, D.; Zhou, Y.; Tao, Y.; Gu, S.; Xu, J.; Deng, Z.; Yin, X.; et al. Poly(Vinylidene Fluoride) Nanofiber Array Films with High Strength for Effective Impact Energy Harvesting. *Energy Technol.* **2021**, *9*, 2100345. [[CrossRef](#)]
143. Rajeev, S.P.; Karimuthil, S.C.; Bhanuprakash, L.; Varghese, S. Flexible nanoenergy harvester using piezo-tribo functional polymer and carbon fibre as electrodes. *Mater. Res. Express* **2018**, *5*, 075509. [[CrossRef](#)]
144. Yang, F.; Zhao, X.; Xue, T.; Yuan, S.; Huang, Y.; Fan, W.; Liu, T. Superhydrophobic polyvinylidene fluoride/polyimide nanofiber composite aerogels for thermal insulation under extremely humid and hot environment. *Sci. China Mater.* **2020**, *64*, 1267–1277. [[CrossRef](#)]
145. Li, K.; Hou, D.; Fu, C.; Wang, K.; Wang, J. Fabrication of PVDF nanofibrous hydrophobic composite membranes reinforced with fabric substrates via electrospinning for membrane distillation desalination. *J. Environ. Sci.* **2019**, *75*, 277–288. [[CrossRef](#)]
146. Kim, H.B.; Yun, C.; Park, C.H. Development of superhydrophobic textiles via polyvinylidene fluoride phase separation in one-step process. *Text. Res. J.* **2018**, *89*, 2595–2603. [[CrossRef](#)]
147. Li, M.; Li, J.; Zhou, M.; Xian, Y.; Shui, Y.; Wu, M.; Yao, Y. Super-hydrophilic electrospun PVDF/PVA-blended nanofiber membrane for microfiltration with ultrahigh water flux. *J. Appl. Polym. Sci.* **2020**, *137*, 48416. [[CrossRef](#)]
148. Rosman, N.; Norharyati Wan Salleh, W.; Asikin Awang, N.; Fauzi Ismail, A.; Jaafar, J.; Harun, Z. Wettability and Surface Area Characteristic of PVDF Nanofibrous Composite Film. *Mater. Today Proc.* **2019**, *19*, 1413–1419. [[CrossRef](#)]
149. Ince Yardimci, A.; Durmus, A.; Kayhan, M.; Tarhan, O. Antibacterial Activity of AgNO₃ Incorporated Polyacrylonitrile/Polyvinylidene Fluoride (PAN/PVDF) Electrospun Nanofibrous Membranes and Their Air Permeability Properties. *J. Macromol. Sci. Part B* **2022**, 1–14. [[CrossRef](#)]
150. Cvek, M.; Mrlík, M.; Osička, J.; Gorgol, D.; Tofel, P. PVDF/PVDF-TRFE blends loaded with BaTiO₃: from processing to performance testing. In Proceedings of the NANOCON Conference Proceedings—International Conference on Nanomaterials, Brno, Czech Republic, 20–22 October 2021; pp. 131–136. [[CrossRef](#)]
151. Mohamadi, S.; Sharifi-Sanjani, N. Crystallization of PVDF in graphene-filled electrospun PVDF/PMMA nanofibers processed at three different conditions. *Fibers Polym.* **2016**, *17*, 582–592. [[CrossRef](#)]
152. Ma, J.; Haque, R.I.; Larsen, R.M. Crystallization and mechanical properties of functionalized single-walled carbon nanotubes/polyvinylidene fluoride composites. *J. Reinf. Plast. Compos.* **2012**, *31*, 1417–1425. [[CrossRef](#)]
153. Kim, M.; Wu, Y.S.; Kan, E.C.; Fan, J. Breathable and Flexible Piezoelectric ZnO@PVDF Fibrous Nanogenerator for Wearable Applications. *Polymers* **2018**, *10*, 745. [[CrossRef](#)]
154. Martins, P.; Costa, C.M.; Benelmekki, M.; Lanceros-Mendez, S. Preparation of magnetoelectric composites by nucleation of the electroactive β -phase of poly(vinylidene fluoride) by NiZnFe₂O₄ nanoparticles. *Sens. Lett.* **2013**, *11*, 110–114. [[CrossRef](#)]
155. Sui, Y.; Wang, Z.; Gao, C. A new synthetical process of PVDF derivatives via atom transfer radical graft polymerizations and its application in fabrication of antifouling and antibacterial PVDF ultrafiltration membranes. *Desalin. Water Treat.* **2014**, *52*, 6377–6388. [[CrossRef](#)]
156. Satapathy, S.; Pawar, S.; Gupta, P.K.; Varma, B.R. Effect of annealing on phase transition in poly(vinylidene fluoride) films prepared using polar solvent. *Bull. Mater. Sci.* **2011**, *34*, 727–733. [[CrossRef](#)]
157. Azzaz, C.M.; C Mattoso, L.H.; Demarquette, N.R.; Zednik, R.J. Polyvinylidene fluoride nanofibers obtained by electrospinning and blowspinning: Electrospinning enhances the piezoelectric β -phase—Myth or reality? *J. Appl. Polym. Sci.* **2021**, *138*, 49959. [[CrossRef](#)]
158. Loizou, K.; Evangelou, A.; Marangos, O.; Koutsokeras, L.; Chrysafi, I.; Yiatros, S.; Constantinides, G.; Zaoutsos, S.; Drakonakis, V. Assessing the performance of electrospun nanofabrics as potential interlayer reinforcement materials for fiber-reinforced polymers. *Compos. Adv. Mater.* **2021**, *30*, 263498332110025. [[CrossRef](#)]
159. Nasir, M.; Matsumoto, H.; Danno, T.; Minagawa, M.; Irisawa, T.; Shioya, M.; Tanioka, A. Control of diameter, morphology, and structure of PVDF nanofiber fabricated by electro-spray deposition. *J. Polym. Sci. Part B Polym. Phys.* **2006**, *44*, 779–786. [[CrossRef](#)]
160. Messiry, M.E. Theoretical analysis of natural fiber volume fraction of reinforced composites. *Alex. Eng. J.* **2013**, *52*, 301–306. [[CrossRef](#)]
161. Wang, H.; Klosterhalfen, B.; Müllen, A.; Otto, T.; Dievernich, A.; Jockenhövel, S. Degradation resistance of PVDF mesh in vivo in comparison to PP mesh. *J. Mech. Behav. Biomed. Mater.* **2021**, *119*, 104490. [[CrossRef](#)] [[PubMed](#)]
162. de Jesus Silva, A.J.; Contreras, M.M.; Nascimento, C.R.; da Costa, M.F. Kinetics of thermal degradation and lifetime study of poly(vinylidene fluoride) (PVDF) subjected to bioethanol fuel accelerated aging. *Heliyon* **2020**, *6*, e04573. [[CrossRef](#)] [[PubMed](#)]

163. Hoa, S.V.; Ouellette, P. Stress corrosion cracking of poly(vinylidene fluoride) in sodium hydroxide. *Polym. Eng. Sci.* **1983**, *23*, 202–205. [[CrossRef](#)]
164. Zhao, X.; Song, L.; Fu, J.; Tang, P.; Liu, F. Experimental and DFT investigation of surface degradation of polyvinylidene fluoride membrane in alkaline solution. *Surf. Sci.* **2011**, *605*, 1005–1015. [[CrossRef](#)]
165. Shinohara, H. Fluorination of polyhydrofluoroethylenes. II. Formation of perfluoroalkyl carboxylic acids on the surface region of poly(vinylidene fluoride) film by oxyfluorination, fluorination, and hydrolysis. *J. Polym. Sci. Polym. Chem. Ed.* **1979**, *17*, 1543–1556. [[CrossRef](#)]
166. Ross, G.J.; Watts, J.F.; Hill, M.P.; Morrissey, P. Surface modification of poly(vinylidene fluoride) by alkaline treatment. I. The degradation mechanism. *Polymer* **2000**, *41*, 1685–1696. [[CrossRef](#)]
167. Awanis Hashim, N.; Liu, Y.; Li, K. Stability of PVDF hollow fibre membranes in sodium hydroxide aqueous solution. *Chem. Eng. Sci.* **2011**, *66*, 1565–1575. [[CrossRef](#)]
168. Tao, X.; Zhou, Y.; Qi, K.; Guo, C.; Dai, Y.; He, J.; Dai, Z. Wearable textile triboelectric generator based on nanofiber core-spun yarn coupled with electret effect. *J. Colloid Interface Sci.* **2022**, *608*, 2339–2346. [[CrossRef](#)]
169. Mhetre, M.R.; Abhyankar, H.K. Human exhaled air energy harvesting with specific reference to PVDF film. *Eng. Sci. Technol. Int. J.* **2017**, *20*, 332–339. [[CrossRef](#)]
170. Wang, Y.J.; Sue, C.Y. Noninvasive Blood Pressure Measurement Using PVDF Fibers Fabricated by NFES and A Photoplethysmography Sensor. *J. Autom. Control. Eng.* **2017**, *7*, 34–38. [[CrossRef](#)]
171. Bifulco, P.; Gargiulo, G.D.; D'Angelo, G.; Liccardo, A.; Romano, M.; Clemente, F.; Cesarelli, M. Monitoring of respiration, seismocardiogram and heart sounds by a PVDF piezo film sensor. In Proceedings of the 20th IMEKO TC4 Symposium on Measurements of Electrical Quantities: Research on Electrical and Electronic Measurement for the Economic Upturn, Together with 18th TC4 International Workshop on ADC and DCA Modeling and Testing, IWADC 2014, Benevento, Italy, 15–17 September 2014; pp. 786–789.
172. Lee, W.K.; Chung, G.S.; Baek, H.J.; Park, K.S. Heart sounds measurement using PVDF film sensor and their comparison with RR intervals of ECG signals. In Proceedings of the IEEE-EMBS International Conference on Biomedical and Health Informatics: Global Grand Challenge of Health Informatics, BHI 2012, Hong Kong, China, 5–7 January 2012; pp. 864–866. [[CrossRef](#)]
173. Åkerfeldt, M.; Lund, A.; Walkenström, P. Textile sensing glove with piezoelectric PVDF fibers and printed electrodes of PEDOT:PSS. *Text. Res. J.* **2015**, *85*, 1789–1799. [[CrossRef](#)]
174. Xin, Y.; Li, X.; Tian, H.; Guo, C.; Sun, H.; Wang, S.; Wang, C. A shoe-equipped piezoelectric transducer system based on PVDF film. *Integr. Ferroelectr.* **2016**, *176*, 140–149. [[CrossRef](#)]
175. Klimiec, E.; Zaraska, W.; Piekarski, J.; Jasiewicz, B. PVDF Sensors—Research on Foot Pressure Distribution in Dynamic Conditions. *Adv. Sci. Technol.* **2013**, *79*, 94–99. [[CrossRef](#)]
176. Lee, D.W.; Jeong, D.G.; Kim, J.H.; Kim, H.S.; Murillo, G.; Lee, G.H.; Song, H.C.; Jung, J.H. Polarization-controlled PVDF-based hybrid nanogenerator for an effective vibrational energy harvesting from human foot. *Nano Energy* **2020**, *76*, 105066. [[CrossRef](#)]
177. Liu, S.; Chen, L.; Zhu, X.; Dai, L.; Xin, Y. Digital piano keyboard based on PVDF piezoelectric film. In Proceedings of the ICALIP 2010—2010 International Conference on Audio, Language and Image Processing, Shanghai, China, 23–25 November 2010; pp. 378–382. [[CrossRef](#)]
178. Sziperlich, P. Piezoelectric A15B16C17 Compounds and Their Nanocomposites for Energy Harvesting and Sensors: A Review. *Materials* **2021**, *14*, 6973. [[CrossRef](#)] [[PubMed](#)]
179. Dai, Y.; Chen, J.; Tian, W.; Xu, L.; Gao, S. A PVDF/Au/PEN Multifunctional Flexible Human–Machine Interface for Multidimensional Sensing and Energy Harvesting for the Internet of Things. *IEEE Sens. J.* **2020**, *20*, 7556–7568. [[CrossRef](#)]
180. Wen, Q.; He, X.; Lu, Z.; Streiter, R.; Otto, T. A comprehensive review of miniaturized wind energy harvesters. *Nano Mater. Sci.* **2021**, *3*, 170–185. [[CrossRef](#)]
181. Viet, N.V.; Wu, N.; Wang, Q. A review on energy harvesting from ocean waves by piezoelectric technology. *J. Model. Mech. Mater.* **2017**, *1*. [[CrossRef](#)]
182. Jbaily, A.; Yeung, R.W. Piezoelectric devices for ocean energy: A brief survey. *J. Ocean. Eng. Mar. Energy* **2015**, *1*, 101–118. [[CrossRef](#)]
183. Gong, T.; Li, T.; Meng, L.; Chen, Y.; Wu, T.; Zhou, J.; Lu, G.; Wang, Z. Fabrication of piezoelectric Ca-P-Si-doped PVDF scaffold by phase-separation-hydration: Material characterization, in vitro biocompatibility and osteoblast redifferentiation. *Ceram. Int.* **2022**, *48*, 6461–6469. [[CrossRef](#)]
184. Dumitrescu, L.N.; Neacsu, P.; Necula, M.G.; Bonciu, A.; Marascu, V.; Cimpean, A.; Moldovan, A.; Rotaru, A.; Dinca, V.; Dinescu, M. Induced Hydrophilicity and In Vitro Preliminary Osteoblast Response of Polyvinylidene Fluoride (PVDF) Coatings Obtained via MAPLE Deposition and Subsequent Thermal Treatment. *Molecules* **2020**, *25*, 582. [[CrossRef](#)] [[PubMed](#)]
185. Kitsara, M.; Blanquer, A.; Murillo, G.; Humblot, V.; De Bragança Vieira, S.; Nogués, C.; Ibáñez, E.; Esteve, J.; Barrios, L. Permanently hydrophilic, piezoelectric PVDF nanofibrous scaffolds promoting unaided electromechanical stimulation on osteoblasts. *Nanoscale* **2019**, *11*, 8906–8917. [[CrossRef](#)]
186. Sun, C.; Guo, Y.; Fang, B.; Yang, J.; Qin, B.; Duan, H.; Chen, Y.; Li, H.; Liu, H. Enhanced Photovoltaic Performance of Perovskite Solar Cells Using Polymer P(VDF-TrFE) as a Processed Additive. *J. Phys. Chem. C* **2016**, *120*, 12980–12988. [[CrossRef](#)]
187. Nie, J.; Zhang, Y.; Dan, M.; Wang, J.; Li, L.; Zhang, Y. Piezophototronic Effect Enhanced Perovskite Solar Cell Based on P(VDF-TrFE). *Solar RRL* **2021**, *5*, 2100692. [[CrossRef](#)]

188. Park, S.; Kim, Y.; Jung, H.; Park, J.Y.; Lee, N.; Seo, Y. Energy harvesting efficiency of piezoelectric polymer film with graphene and metal electrodes. *Sci. Rep.* **2017**, *7*, 17290. [[CrossRef](#)] [[PubMed](#)]
189. Kargar, S.M.; Hao, G. An Atlas of Piezoelectric Energy Harvesters in Oceanic Applications. *Sensors* **2022**, *22*, 1949. [[CrossRef](#)]
190. Koç, M.; Paralı, L.; Şan, O. Fabrication and vibrational energy harvesting characterization of flexible piezoelectric nanogenerator (PEN) based on PVDF/PZT. *Polym. Test.* **2020**, *90*, 106695. [[CrossRef](#)]
191. Bae, J.; Song, J.; Jeong, W.; Nandanapalli, K.R.; Son, N.; Zulkifli, N.A.B.; Gwon, G.; Kim, M.; Yoo, S.; Lee, H.; et al. Multi-deformable piezoelectric energy nano-generator with high conversion efficiency for subtle body movements. *Nano Energy* **2022**, *97*, 107223. [[CrossRef](#)]
192. Zhang, Y.; Lu, R.; Zhang, S.; Tang, B. Intelligent light-driven flexible solar thermoelectric system. *Chem. Eng. J.* **2021**, *423*, 130260. [[CrossRef](#)]
193. Han, S.; Chen, S.; Jiao, F. Insulating polymers for flexible thermoelectric composites: A multi-perspective review. *Compos. Commun.* **2021**, *28*, 100914. [[CrossRef](#)]
194. Kumar, A.; Kumar, R.; Satapathy, D.K. Bi₂Se₃-PVDF composite: A flexible thermoelectric system. *Phys. B Condens. Matter* **2020**, *593*, 412275. [[CrossRef](#)]
195. Li, X.; Cai, K.; Gao, M.; Du, Y.; Shen, S. Recent advances in flexible thermoelectric films and devices. *Nano Energy* **2021**, *89*, 106309. [[CrossRef](#)]
196. Wang, J.; Xiao, F.; Zhao, H. Thermoelectric, piezoelectric and photovoltaic harvesting technologies for pavement engineering. *Renew. Sustain. Energy Rev.* **2021**, *151*, 111522. [[CrossRef](#)]
197. Dun, C.; Hewitt, C.A.; Huang, H.; Montgomery, D.S.; Xu, J.; Carroll, D.L. Flexible thermoelectric fabrics based on self-assembled tellurium nanorods with a large power factor. *Phys. Chem. Chem. Phys.* **2015**, *17*, 8591–8595. [[CrossRef](#)] [[PubMed](#)]
198. Paulraj, I.; Lourduhamsy, V.; Liu, C.J. Organic/Inorganic n-type PVDF/Cu_{0.6}Ni_{0.4} hybrid composites for thermoelectric application: A thermoelectric generator made of 8 pairs of p-leg ZnSb/Sb and n-leg β-PVDF/Cu_{0.6}Ni_{0.4}. *Chem. Eng. J.* **2022**, *446*, 137083. [[CrossRef](#)]
199. Hu, S.; Zeng, S.; Li, X.; Jiang, J.; Yang, W.; Chen, Y.; Li, M.; Zheng, J. Flexible and high performance of n-type thermoelectric PVDF composite film induced by nickel nanowires. *Mater. Des.* **2020**, *188*, 108496. [[CrossRef](#)]
200. Park, D.; Kim, M.; Kim, J. High-performance PANI-coated Ag₂Se nanowire and PVDF thermoelectric composite film for flexible energy harvesting. *J. Alloys Compd.* **2021**, *884*, 161098. [[CrossRef](#)]
201. Park, D.; Ju, H.; Kim, J. Enhanced thermoelectric properties of flexible N-type Ag₂Se nanowire/polyvinylidene fluoride composite films synthesized via solution mixing. *J. Ind. Eng. Chem.* **2021**, *93*, 333–338. [[CrossRef](#)]
202. Zhang, Y.; Rhee, K.Y.; Park, S.J. Facile design of a domestic thermoelectric generator by tailoring the thermoelectric performance of volume-controlled expanded graphite/PVDF composites. *Compos. Part B Eng.* **2019**, *176*, 107234. [[CrossRef](#)]
203. Chen, Y.; He, M.; Tang, J.; Bazan, G.C.; Liang, Z. Flexible Thermoelectric Generators with Ultrahigh Output Power Enabled by Magnetic Field-Aligned Metallic Nanowires. *Adv. Electron. Mater.* **2018**, *4*, 1800200. [[CrossRef](#)]
204. Kim, M.S.; Jo, S.E.; Ahn, H.R.; Kim, Y.J. Modeling of a honeycomb-shaped pyroelectric energy harvester for human body heat harvesting. *Smart Mater. Struct.* **2015**, *24*, 065032. [[CrossRef](#)]
205. Chen, W.Y.; Shi, X.L.; Zou, J.; Chen, Z.G. Wearable fiber-based thermoelectrics from materials to applications. *Nano Energy* **2021**, *81*, 105684. [[CrossRef](#)]
206. Na, Y.; Kim, S.; Mallem, S.P.R.; Yi, S.; Kim, K.T.; Park, K.I. Energy harvesting from human body heat using highly flexible thermoelectric generator based on Bi₂Te₃ particles and polymer composite. *J. Alloys Compd.* **2022**, *924*, 166575. [[CrossRef](#)]
207. Kumar, S.; Singh, H.H.; Khare, N. Flexible hybrid piezoelectric-thermoelectric generator for harnessing electrical energy from mechanical and thermal energy. *Energy Convers. Manag.* **2019**, *198*, 111783. [[CrossRef](#)]
208. Pan, J.; Li, Y.; Guo, G.; Zhao, X.; Yu, J.; Li, Z.; Xu, S.; Man, B.; Wei, D.; Zhang, C. Synergizing piezoelectric and plasmonic modulation of PVDF/MoS₂ cavity/Au for enhanced photocatalysis. *Appl. Surf. Sci.* **2022**, *577*, 151811. [[CrossRef](#)]
209. Banerjee, S.; Bairagi, S.; Ali, S.W. A lead-free flexible piezoelectric-triboelectric hybrid nanogenerator composed of uniquely designed PVDF/KNN-ZS nanofibrous web. *Energy* **2022**, *244*, 123102. [[CrossRef](#)]
210. Lee, Y.H.; Kim, D.H.; Kim, Y.; Shabbir, I.; Li, M.; Yoo, K.H.; Kim, T.W. Significant enhancement of the output voltage of piezoelectric/triboelectric hybrid nanogenerators based on MAPbBr₃ single crystals embedded into a porous PVDF matrix. *Nano Energy* **2022**, *102*, 107676. [[CrossRef](#)]
211. Mallick, Z.; Saini, D.; Sarkar, R.; Kundu, T.K.; Mandal, D. Piezo-phototronic effect in highly stable lead-free double perovskite Cs₂SnI₆-PVDF nanocomposite: Possibility for strain modulated optical sensor. *Nano Energy* **2022**, *100*, 107451. [[CrossRef](#)]
212. He, Y.; Wang, H.; Sha, Z.; Boyer, C.; Wang, C.H.; Zhang, J. Enhancing output performance of PVDF-HFP fiber-based nanogenerator by hybridizing silver nanowires and perovskite oxide nanocrystals. *Nano Energy* **2022**, *98*, 107343. [[CrossRef](#)]